DOI:10.14753/SE.2023.2889

SEMMELWEIS EGYETEM

DOKTORI ISKOLA

Ph.D. értekezések

2889.

SZÉKELY TAMÁS

Onkológia
című program

Programvezető: Dr. Bödör Csaba, egyetemi tanár

Témavezetők: Dr. Krenács Tibor, kutatóprofesszor

DOI:10.14753/SE.2023.2889

STROMAL GROWTH RELATED BIOMARKER AND MATRIX PROTEIN EXPRESSION IN PRIMARY MYELOFIBROSIS IN RELATION TO GÖMÖRI'S SILVER GRADING

PhD thesis

Tamás Székely MD

Doctoral School of Pathological Sciences

Semmelweis University

Supervisor: Tibor Krenács, PharmD, DSc

Official reviewers: Béla Kajtár, MD, PhD and Deján Dobi, MD, PhD

Head of the Comprehensive Exam Committee: Miklós Kellermayer, MD, DSc

Members of the Comprehensive Exam Committee: Pál Maurovich-Horváth, MD, DSc

Miklós Kozlovszky, PhD

Budapest

2023

DOI:10.14753/SE.2023.2889

TABLE OF CONTENTS

DOI:10.14753/SE.2023.2889

DOI:10.14753/SE.2023.2889

LIST OF ABBREVIATIONS

ASXL1	Additional Sex Combs-like protein 1
ASXL1	Additional Sex Combs-like protein 1
bFGF	Basic fibroblast growth factor
BM	Bone marrow
BMF	Bone marrow fibrosis
CD34	Cluster of Differentiation 34 protein
CEL	Chronic eosinophilic leukemia
CML	Chronic myeloid leukemia
CNL	Chronic neutrophilic leukemia
Cx43	Connexin 43 protein
CXCL12	Stromal cell-derived factor-1 chemochine
CXCR4	Receptor for the chemokine CXCL12
DAB	3,3'-diaminobenzidine
DIPSS	Dynamic International Prognostic Scoring System
DIPSS-Plus	Dynamic International Prognostic Scoring System Plus
DNA	Deoxyribonucleic Acid
EC	European Consensus
ERK	Extracellular Signal-Regulated Kinase
ERK/MAPK	Extracellular Signal-Regulated Kinase/Mitogen-Activated Protein Kinase signaling pathway
ET	Essential thrombocythemia
ETT TUKEB	National Committee for Research Ethic
EZH2	Enhancer of Zeste Homolog 2 protein
FGF	Fibroblast Growth Factor
HE	Hematoxylin Eosin
IDH1	Isocitrate Dehydrogenase 1
IL-1	Interleukin 1
JAK	Janus kinase
JMML	Juvenile myelomonocytic leukemia
L-NGFR	Low-affinity Nerve Growth Factor Receptor
MAPK	Mitogen-Activated Protein Kinase signaling pathway
MF-0	Myelofibrosis , grade 0
MF-1	Myelofibrosis , grade 1
MF-2	Myelofibrosis , grade 2
MF-3	Myelofibrosis , grade 3
MPL	Thrombopoietin receptor (myeloproliferative leukemia protein)
MPN	Myeloproliferative neoplasms

DOI:10.14753/SE.2023.2889

NGF	Nerve Growth Factor
PDGF	Platelet-Derived Growth Factor
PDGF	Platelet-Derived Growth Factor receptor
phospho-ERK1-2	phosphorylated forms of Extracellular Signal-Regulated Kinase 1 and 2
PI3K/Akt	Phosphatidylinositol 3-Kinase/Protein Kinase B (also known as Akt) signaling pathway
PMF	Primary myelofibrosis
PV	Polycythemia vera
RBC	Red blood cells
RTK	Receptor Tyrosine Kinase
SR3B1	Splicing factor 3b subunit 1 coding gene
SRSF2	Serine and Arginine Rich Splicing Factor 2
STAT	Signal transducer and activator of transcription
TET2	Ten-Eleven-Translocation-2 gene
TGF-ß	Transforming Growth Factor Beta
TrkA	Tropomyosin receptor kinase A
VEGF	vascular endothelial growth factor
WHO	World Health Organization
WMA	World Medical Association

DOI:10.14753/SE.2023.2889

1 INTRODUCTION

1.1 Primary myelofibrosis

Having the potential to self-renew, pluripotent hematopoietic stem cells can develop into mature blood cells such as red blood cells (RBC), lymphocytes, granulocytes, megakaryocytes, and macrophages from either the lymphoid or myeloid lineage. The bone marrow (BM) environment, growth factors, and transcription factors all have major influences on the hematopoietic maturation process. In addition to these variables, clonal genetic modifications are crucial for the regulation of maturation and proliferation processes in hematopoiesis.

Myeloproliferative neoplasms are a diverse collection of diseases caused by the abnormal development of myeloid cell lines[1]. Primary myelofibrosis (PMF) is a member of the myeloproliferative neoplasms (MPN) characterized by aberrant clonal stem cell-derived myeloproliferation. Chronic myeloid leukemia (CML), chronic neutrophilic leukemia (CNL), chronic eosinophilic leukemia (CEL), essential thrombocythaemia (ET), polycythemia vera (PV), juvenile myelomonocytic leukemia (JMML) are other conditions that fall within the MPN umbrella. While CML is a Philadelphia chromosome (*BCR::ABL1*) positive disease , PMF, ET, and PV are *BCR::ABL1*-negative MPNs [1]. All of these neoplasms are characterized by clonal myeloid lineage growth and in PMF an increased stromal cell activation. By overproducing extracellular matrix as a result of stromal cell activation, the bone marrow space shrinks, which physically compromises hemopoiesis. Certain genetic mutations are present in PMF. Driver mutation in the Janus kinase 2 (*JAK2*), Calreticulin (*CALR*), or proto-oncogene, thrombopoietin receptor (MPL) is present in roughly 90% of PMF patients. Less commonly, mutations of additional clonal markers (such as *ASXL1, EZH2, TET2, IDH1/2, SRSF2 and SR3B1*) are also involved[2]. Functional modification of the JAK binding cytokine receptor is the common final consequence of genotypical alterations. Deregulated overproduction and release of pro-inflammatory cytokines (such as IL-1, TGF-ß), growth factors (such as bFGF, PDGF, and VEGF), and extracellular matrix components (fibronectin, laminin and collagens) are caused by constitutive JAK-STAT signaling, which is triggered by abnormal receptors. These chemical factors' secondary effects on the bone marrow matrix

have been directly linked to the development of fibrosis and osteosclerosis. Increased cytokine-directed signaling, increased activation of the ERK/MAPK and PI3K/Akt pathways, as well as the action of chemicals released upon neutrophil engulfment that have dysregulated receptor activity, all contribute to increased synthesis of connective tissue fibers [2]. In fibroblast activation, increased production and release of platelet-derived growth factor (PDGF), fibroblast growth factor receptor (FGF), transforming growth factor beta (TGFβ) and vascular endothelial growth factor (VEGF) play important roles (see Figure 1.).

1.2 Epidemiology

The incidence of PMF, fibrotic stage, is expected to range between 0.44 and 1.5 instances per 100,000 person-years [3,4]. Men and women are approximately equally affected by PMF. It is most prevalent in the sixth and seventh decades of life, and less than 10% of overt PMF cases are diagnosed in people under the age of 40. The disease rarely affects children [5].

1.3 Subtypes, clinical stages

Primary myelofibrosis, prefibrotic stage (referred also as pre-MF). This represent hypermetabolic stage with hypercellular bone marrow.

Primary myelofibrosis, overt fibrotic stage (referred also as MF, PMF). This stage represents a fibrotic, hypocellular, osteosclerotic bone marrow structure with decreased functionality (see Table 2).

1.4 Clinical features

PMF is a condition that is more aggressive than ET, PV, and pre-MF. It is progressive and has a dramatic impact on the patients' quality of life. Patients with ET, PV, or pre-MF run the risk of developing myelofibrosis, which may be referred to as post-ET-MF, post-PV-MF, etc. Patients with PMF have more mutations, cytogenetic abnormalities, and a higher likelihood of leukemic transformation [6]. Up to one-third of patients are asymptomatic at the time of diagnosis, and many of these people are identified when

unrelated blood tests reveal minor abnormalities, such as anemia and thrombocytopenia [7].

Hypermetabolic conditions manifesting as fevers, anorexia, weight loss, nocturnal sweats, weariness, bone discomfort, and spleen-related symptoms like pain and early satiety, are frequently present in many cases. Thrombosis and bleeding are also common symptoms in patients with PMF. Anaemia is common, especially in the later stages, and it frequently coexists with thrombocytopenia [7]. Leukemic transformation occurs in 20-25% of patients and is characterized by the presence of 20% blasts in blood or bone marrow for an extended period of time [8].

1.5 Diagnostic Criteria for Primary Myelofibrosis diagnosis

A number of different conditions related to both hematological and non-hematological diseases have been linked to consequential bone marrow fibrosis. A correct diagnosis of PMF requires a BM biopsy, cytogenetic analysis, specific hematological and laboratory processing, and clinical evaluation to rule out a secondary myelofibrotic process. According to the revised World Health Organization (WHO) [9], all three major criteria plus at least one minor criteria must be met to establish a diagnosis of PMF

Table 1 Major and minor diagnostic criteria for primary myelofibrosis according to 2016 revised World Health Organization (WHO) [9]

	Major criteria
1	Typical megakaryocyte changes, accompanied by ≥ grade 2 reticulin/collagen fibrosis
2	The presence of *JAK2*, *CALR* or *MPL* mutations, or the presence of other clonal markers, or absence of evidence for reactive bone marrow fibrosis
3	Not meeting WHO criteria for other myeloid neoplasms
Minor criteria	
Anemia not otherwise explained	
Leukocytosis ≥ 11 × 109/L	
Palpable splenomegaly	

Increased serum lactate dehydrogenase
A leukoerythroblastic blood smear (in overtly fibrotic PMF only)

1.6 Grading and scoring myelofibrosis

1.6.1 Grading myelofibrosis

Myelofibrosis development and progression is a gradual, sequential process. In addition to a number of other factors, the disease's prognosis depends on the degree of bone marrow fibrosis (BMF). There are many grading protocols available to describe the feature of increased reticulin fiber and, in certain situations, collagen fiber deposition. Methods of assessing and rating BMF rely mainly on manual procedure evaluation under a light microscope. The most common is a four-point scale (0–3) system used by the European Consensus (EC) for grading bone marrow fibrosis based on the density of the reticulin network, fiber localization, the collagen network, and osteosclerosis [9]. Classification based on histology ranges from grade 0 to grade 3. (MF-0; MF-1; MF-2; M-3). According to the 5th edition of the WHO classification of haematolymphoid tumors, there are two subtypes of PMF: prefibrotic, which includes histological grades MF-0 and MF-1, and fibrotic, which includes histological grades MF-2 and MF-3 (Table 2) [9].

Table 2 Histological grading (MF-0; MF-1; MF-2; M-3) of bone marrow fibrosis based on the EC consensus and subtypes of PMF based on 2022 edition of WHO classification of haematolymphoid tumors 9, 10

WHO subtype	*Histological grade*	*Bone marrow histology*
Prefibrotic	*MF-0*	Only perivascular reticulin fragments with no intersections
	MF-1	Focal, loose reticulin network with mainly perivascular intersections
Fibrotic	*MF-2*	Paratrabecular or central deposition of dense reticulin with regular intersections and occasional collagen bundles
	MF-3	Diffuse and dense intersecting reticulin meshwork and collagen bundles with osteosclerosis

1.6.2 Grading procedure

The diagnosis and grading of BMF are still mainly performed using microscopic evaluation. Histological evaluation of myelofibrosis is semi-quantitative, based on Gömöri's silver staining, and requires not only strictly regulated laboratory processing but also experienced hematopathologists. Due to a number of influencing factors such as preanalytical conditions, staining variables, a lack of a positive staining internal standard, and of course diagnostic subjectivity, standardization of the selective silver impregnation is rather difficult. Inter-rater differences might be large when it comes to grade evaluation. To objectively quantify BMF, computer-assisted image analysis is being used more often in clinical studies as an auxiliary to semi-quantitative grading in addition to human evaluation. Computer-assisted image analysis has been proven to be more accurate than regular histology in detecting BMF level changes in MF patients receiving therapy, and it also correlates well with morphology [11].

1.6.3 Scoring of myelofibrosis

Aside from the BMF grade, there are other, primarily clinical factors that may influence the course of the illness. The most widely used prognostic scoring model for predicting survival is the Dynamic International Prognostic Scoring System (DIPSS). There are five risk variables used, such as patient age, symptoms, anemia, leukocytosis, and the presence of circulating blasts. In order to predict overall median survival in PMF patients, the DIPSS-Plus scoring system extends prognostic data by karyotype, platelet count, and transfusion status. Low, intermediate-1, intermediate-2, and high risk groups exist based on the cumulative point calculation [12]. Figure 1. shows the difference in disease outcome linked to risk categories using the DIPSS-Plus system in a study that involved 428 PMF patients [13].

DOI:10.14753/SE.2023.2889

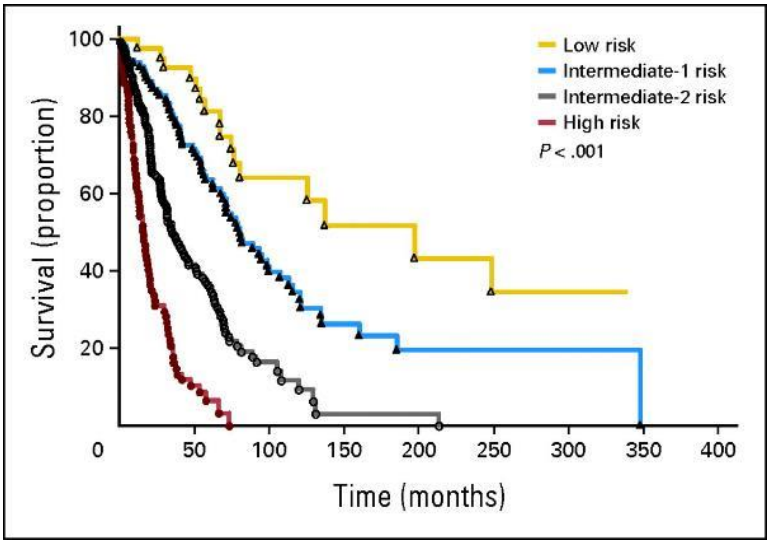

Figure 1* Survival data from 428 patients with primary myelofibrosis who were assessed within a year of diagnosis and stratified by the Dynamic International Prognostic Scoring System (DIPSS) + karyotype + platelet count + transfusion status prognostic scores. Low risk, zero adverse points; n = 46; median survival, approximately 180 months. Intermediate-1 risk, one adverse point; n = 114; median survival, approximately 80 months. Intermediate-2 risk, two or three adverse points; n = 177; median survival, approximately 35 months. High risk, four to six adverse points; n = 91; median survival, approximately 16 months. Scale for DIPSS: high risk, three adverse points; intermediate-2, two adverse points; intermediate-1, unfavorable karyotype, platelets < 100 x 109/L, and transfusion need, one adverse point

**The figure is from on article by Naseema Gangat et al. "DIPSS Plus: A Refined Dynamic International Prognostic Scoring System for Primary Myelofibrosis That Incorporates Prognostic Information From Karyotype, Platelet Count, and Transfusion Status"* [13.]

1.7 Stromal cell growth related biomarkers involved in PMF

L-NGFR, phospho-ERK1-2, and CXCL12 are important stromal cell growth-related biomarkers that may potentially be involved in PMF progression. These biomarkers are mostly found in the stromal cells of the bone marrow. They may play a big role in activating fibroblasts, which is what leads to more pathogenic matrix formation. Low affinity nerve growth factor receptor (L-NGFR)

1.7.1 L-NGFR

Low affinity nerve growth factor receptor (L-NGFR; CD271, or referred to as p75 neurotrophin receptor - p75NTR), an unusual member of the tumor necrosis factor superfamily, has long been detected in the bone marrow stromal cell network [14]. L-NGFR has been involved in the regulation of neuronal survival and apoptosis but it can also act as a tyrosin kinase co-receptor for the anti-apoptotic tropomyosin receptor kinase A (TrkA) to enhance MAPK pathway activation, culminating in ERK1-2 phosphorylation and nuclear translocation [15, 16]. Both L-NGFR expression and NGF-TrkA signaling can support bone and bone marrow mesenchymal stem cell (MSc) development [17, 18]. In addition, TrkA upregulation can enhance the survival and regenerative capacity of bone marrow stromal stem cells through upregulation of the Erk/Bcl-2 pathway [19]. In myelofibrotic bone marrow MAPK activation can also be induced through receptor tyrosin kinase signaling i.e. PDGFR by PDGF overproduced by pathological megakaryocytes, as one of the major driving forces of fibroblast activation [20]. In line with this, PDGFR-β expression in the stromal network showed close correlation with the silver impregnation based myelofibrosis grades [21-23].

1.7.2 CXCL12 – CXCR4 receptor

The chemokine CXCL12 (stromal cell-derived factor 1 - SDF1, or C-X-C motif chemokine 12), produced by stromal and endothelial cells and osteoblasts, plays an important role in maintaining stem cell quiescence by safeguarding both the perivascular and endosteal bone marrow niches [24]. Its receptor CXCR4 is known to be expressed in CD34+/c-kit+ hemopoietic progenitors and leukemic blasts. Mesenchymal stromal cells can resist radiation-induced cell death and the CXCL12 (SDF1)-CXCR4 signaling within the stromal microenvironment promotes niche regeneration during stem cell transplantation [25]. Bone marrow stromal cells, as a dynamic syncytium, communicate via Cx43 (and Cx45) gap junctions, which are required for proper CXCL12 secretion and hematopoietic stem cell homeostasis [26]. Accordingly, inhibition of gap junctions impairs CXCL12 secretion and the homing of CD34+ bone marrow progenitors. Our group has previously demonstrated the upregulation of Cx43 gap junctions in leukemic tumor samples, characterized by an increased stromal/hematopoietic cell ratio [27].

The CXCL12/CXCR4 pathway can be induced by oncogenic *JAK2*, which frequently suffers activating mutations in primary myelofibrosis, and *JAK2* inhibition can reduce the chemotaxis of hemopoietic cells isolated from primary myelofibrosis [28]. A subpopulation of leukemic cells with stem cell-like features can maintain tumor growth by escaping antitumor therapies and repopulating the tumor [29]. Myelofibrosis, characterized by increased stromal cell activation, may also involve CXCL12 upregulation, which can contribute to protecting leukemic stem cells [30].

1.8 Extracellular matrix components in PMF

Type I and type III collagens as well as fibrillin-1 structure are core components of the overproduced fiber network. Although sporadic papers in a small number of cases suggested a link between serum type III procollagen levels and reticulin fibrosis [31] or in situ type III procollagen levels and reticulin fibrosis [32], fibrosis-related matrix protein production along the development of myelofibrosis had not been studied in detail before our work.

1.8.1 Type I and type III collagen

Regenerative organ fibrosis is associated with increased type I and type III collagen synthesis and deposition [33, 34]. A similar path is present in bone marrow fibrosis. A localized, loose network of reticular fibers with infrequent, perivascular crossings forms at the start of myelofibrosis. The skeleton of reticular fibers is composed of homotrimeric type III collagen fibrils [34-36 37]. While osteoblasts (and osteocytes) primarily deposit type I collagen in the bone matrix, these may also aid in organizing and regulating its diameter during fibrillogenesis [38]. In addition to rising collagen fiber density and a rise in the frequency of crossings between reticular and accumulating type I collagen fibers, advanced myelofibrosis (MF-2) is characterized by early bundle formation [39]. Following this, there is an acceleration of osteosclerosis (MF-3) and an increase in reticulin concentration and collagen deposition.

1.8.2 Fibrillin-1

Fibrillin-1 is an evolutionarily conserved extracellular matrix glycoprotein. It is well known for serving as a template framework in the construction of elastic fiber and is the

main constituent of microfibril polymers with a diameter of 10–12 nm [40]. The microfibrils, which are components of the fibrillin-1 and fibrillin-2 isotypes, are responsible for granting stretch tolerance to elastic tissues including arteries and ligaments [41]. In elastin-free matrix architectures, the microfibrils also offer mechanical robustness. The presence of an excessive extracellular matrix, primarily made up of type I and type III collagens [41] as well as a disorganized fibrillin-1 deposition in scleroderma [42], which is brought on by congenital dysfunctions of the fibrillin-1 protein, highlight their roles in fibrotic conditions [42].

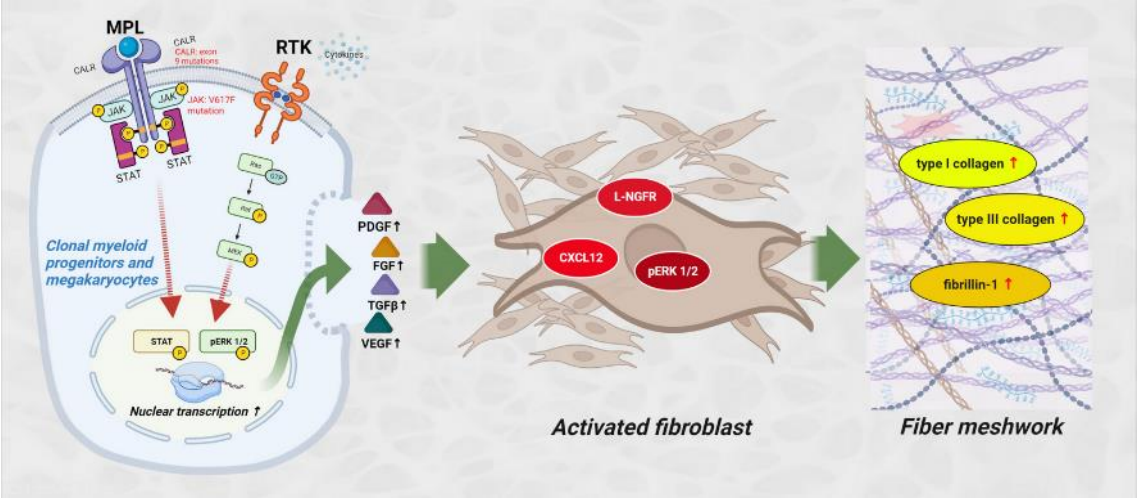

Figure 2. The main mechanism of primary myelofibrosis progression. Clonal myeloid progenitors and megakaryocytes activated by Calreticulin, JAK-mutated MPL receptor, or increased cytokine-directed signaling via RTK, play an important role in fibroblast activation. Fibrosis is facilitated by the overproduction of PDGF, FGF, TGFb, and VEGF by clonal cells which activate fibroblasts. We tested the expression of L-NGFR, CXCL12, and pERK1/2 produced by stromal cells, as well as type I and type III collagens, and fibrillin-1, which occur both in the stromal cell and the extracellular matrix scaffolding throughout the bone marrow. *Created with BioRender.com*

DOI:10.14753/SE.2023.2889

2 OBJECTIVES

1. The main objective of this study was to find connections between the expression of stromal cell growth-related biomarkers and fibrosis-related extracellular matrix proteins and the traditional Gömöri's silver impregnation-based myelofibrosis grades.

2. L-NGFR receptor, CXCL12 motif chemokin, and phospho-ERK1-2 signal transducer expression were examined using immunohistochemistry in PMF cases of different silver grades. Our goal was to identify which marker shows the strongest statistically significant correlation with the histological grade obtained using Gömöri's staining.

3. Major extracellular matrix proteins involved in regenerative fibrosis including type I collagen, type-III collagen and fibrillin-1 were selected for immunohistochemical labeling. Our goal was also to determine the correlation of matrix production by stromal cells with histological grades determined by Gömöri's silver staining, and to identify the biomarker with the strongest and statistically most significant association with MF grades.

4. Our additional objective was to develop an immunoreaction-based, computer-assisted, semi-automated digital image quantification method using a commercially available computer algorithm. We sought to demonstrate if this approach can accurately reproduce and, perhaps in the future, replace Gömöri's silver staining-based grading when set up using eye-control.

3 METHODS

3.1 Bone marrow samples

Our cohort included Jamshidi biopsies of patients diagnosed with primary myelofibrosis at the 1st Department of Pathology, Semmelweis University, between 2016 and 2022. The selection of samples was based on pathological diagnoses. It was followed by the collection of paraffin blocks and Hematoxylin Eosin (HE) stained slides from the archive. A quick review was done to make sure that the quality and number of samples in the block were good and enough for the study to begin. There was no repeated HE staining, however, Gömöri's reticular fiber staining was performed again in all cases that were selected for analysis to confirm or supervise the original grading. The study was divided into two parts. The samples used for the analysis of stromal cell receptors and matrix components varied slightly. Firstly the expression of L-NGFR, phospho-ERK1-2, and CXCL12 were studied, later he type I, type III, and fibrillin-1 were marked and evaluated on an extended sample collection. A total of 60 and 68 samples were studied in the first and the second part of the study, respectively. Due to the consumption of tissue within the paraffin blocks, some sample had to be replaced by new ones selected from the same grade group. MF-0 grade group samples were expanded with 5 additional cases for the second sample set. And also, an additional 5 non-myelofibrotic, non fibrotic bone marrow samples were selected as negative controls for the second part of the study.

In the first part of the study, 36 cases were grade 3 (MF-3) (22 males, 14 females; median age 66.3 years; range 45-86), 18 cases as grade 2 (MF-1) (5 males, 13 females; median age 56.2 years; range 31-76) and 6 cases were diagnosed as prefibrotic myelofibrosis with grade 1 (MF-1) fibrosis (3 males, 3 females; median age 54.1 years; range 29-86). Forty-eight patients (80%) carried either the *JAK2 V617F* mutation (43 out of 60; 4 MF-1, 13 MF-2 and 26 MF-3 cases; 71,7%) or *CALR* mutations (5 out of 60; 2 MF-2 and 3 MF-3 cases; 8,3%). Four out of 5 patients harbored type 1 and 1 patient had a type 2 *CALR* mutation. Twelve patients (20%) were double negative for the *JAK2* and *CALR* analyses.

In the samples of the second study part, 36 cases were confirmed to be MF-3 (20 males, 16 females; median age 66 years; range 45-86), 16 to be MF-2 (5 males, 11 females;

median age 59 years; range 31-76), 6 to be MF-1 (2 males, 4 females; median age 46.5 years; range 29-69), and 5 were MF-0 pre-fibrotic based on atypical megakaryocytes and megakaryocytic and granulocytic proliferation [43] (2 males, 3 females; median age 39 years; range 15–82) (**Table 3**). Five samples with non-myelofibrotic (structurally normal) bone marrow morphology were also included as controls (2 males, 3 females; median age 52 years; range 44-79). *JAK2 V617F* or *CALR* mutations were detected in 52 of the 63 PMF patients (82,5%). *JAK2 V617F* mutation was found in 45 patients (71,4%) (2 MF-0, 5 MF-1, 12 MF-2 and 26 MF-3) and *CALR* mutations were detected in 7 patients (11,1%) (2 MF-0, 2 MF-2 and 3 MF-3 cases; 3/7 had type-1 and 1/7 had type-2 and 3/7 had other *CALR* mutations). 11 patients (17,5%) were double negative.

Table 3. Table shows case numbers, male (M) and female (F) ratio in each group in both parts of the study

	Control	*MF-0*	*MF-1*	*MF-2*	*MF-3*	*ALL*
First part	-	-	6 (M:3;F:3)	18 (M:5; F:13)	36 (M:22; F:14)	60
Second part	5 (M:2; F:3)	5 (M:2; F:3)	6 (M:2; F:4)	16 (M:5;F:11)	36 (M:20; F:16)	68

Gömöri's silver staining was used to determine the grade of MF [44]. These results served as the classification basis for our samples. For regular Gömöri's reticular fiber staining, rehydrated slides were treated with 1% potassium permanganate for 2 minutes of oxidation, 2% potassium metabisulphite for 1 minute of decolorization, 2% ferric ammonium sulfate for 1 minute of curing, and 10% silver nitrate with 2% potassium hydroxide for 1 minute of silver impregnation. Sequential treatments in 10% formalin for 5 minutes, 0.02% gold chloride for 10 seconds, 2% potassium metabisulfite for 1 minute, and finally 1% sodium thiosulfate for 1 minute were used to complete the staining process. After dehydrating, the sections were mounted after being washed in distilled water between incubation steps[44].

The procedure of diagnostic reticulin grading followed the European Consensus set up for bone marrow fibrosis [45] (Table 2).

The study was conducted in accordance with the Helsinki Declaration. Our study was performed in line with the regulations of the WMA Declaration of Helsinki and was approved by the National Committee for Research Ethics (ETT TUKEB) under the number IV/129/2022/EKU.

3.2 Automated immunohistochemical staining

For immunohistochemistry, 3 μm thick sections mounted on adhesive glass slides were heat activated for >2 h at 62 ºC and dewaxed after reaching room temperature. Immunostaining, except for CXCL12, was done using the Ventana Bechmark Ultra automated system (Roche Diagnostics, Tucson, AR) including antigen retrieval for 40 min in the high pH CC1 buffer, incubation with the primary antibodies for 60 min and then with the Ultraview detection system for 40 min, and visualization using DAB/hydrogen peroxide development. CXCL12 was detected with manual immunostaining after TRIS-EDTA retrieval (pH 9) for 40 min, using the same incubation times as in the automated system with peroxidase conjugated Histols micropolymer (Histopathology Kft, Pécs) and revealed with the DAB Quanto (TA-060-PHDX, Thermo Sci. Runcon, UK) kit. All immunoreactions were completed with nuclear counterstaining using hematoxylin. Primary antibodies used were monoclonal mouse anti-human p75 low affinity nerve growth factor receptor (L-NGFR, 1:100, clone: 7F10, Leica-NovoCastra, Newcastla, UK), CXCL12/SDF-1α (1:50, clone:#79018, R&D, Minneapolis, MN, USA), rabbit anti-phospho-ERK1-2 (p44/42; Thr202/Tyr204; 1:100, clone:20G11, Cell Signaling, Danvers, MA, USA), as well as rabbit polyclonal connexin 43 (Cx43, 1:100, #3512, Cell Signaling). In addition, the rabbit anti-Cx43 (1:100) and the mouse anti-L-NGFR (1:100) primary antibodies were simultaneously combined in 10 cases of myelofibrosis for double immunofluorescence, and detected using a mixture of Alexa Fluor 488 (green, 1:200) or Alexa Fluor 546 (red, 1:200) conjugated goat anti-mouse/or -rabbit (IgG H + L) antibodies (both Invitrogen/-Life Technologies, Eugene, OR, USA), for 90 min incubations at each sequence. Cell nuclei were revealed in blue using the DNA staining Hoechst (bisbenzimide,1:500; Sigma-Aldrich, St. Louis, MO, USA) fluorescing dye for 1 min., and finally the sections were coverslipped with fluorescent mounting medium (Dako). For matrix protein labeling the following primary antibodies were used: rabbit polyclonal anti-human type I collagen (1:1000, # PA5-95137, Thermo-

Fisher/Invitrogen, Waltham, MA), anti-mouse/human type III collagen (1:100, # 600-401-105-01, Thermo-Fisher/Rockland); and mouse monoclonal anti-human fibrillin-1 (1:800, IgG1, clone:26, MAB2502, Merck/Chemicon, Darmstadt, Germany) and CD34 (1:100, IgG1, clone: QBEnd/10, Merck-Sigma-Aldrich) and IgG-s. After hematoxylin counterstaining, dehydration and clearing the sections were mounted using Pertex medium.

3.3 Scoring and image analysis using digital whole slides

With the help of a Pannoramic 1000 Scanner (3DHistech Ltd., Budapest), all stained slides used in this study were subjected to whole slide digitalization. Visual analysis on high resolution monitors and scoring of each staining series were then performed using the SlideViewer program (3DHistech). A similar methodology to that used to evaluate Gömöri's reticulin staining was applied to evaluate the extracellular matrix immunoreactions. Score 0: only infrequent, fragmented fibrils with no intersections; Score 1: focal, loose networks with only perivascular intersections; Score 2: medium density of positive fibrils with regular intersections and some extrafibrillar deposition; Score 3: diffuse, densely intersecting fibril networks and more extrafibrillar antigen deposition.

Fibrillin-1 immunoreaction series was selected for digital image analysis. The QuantCenter software package's PatternQuant module (3DHistech), a semi-automated machine learning algorithm, was used for the image analysis. Each slide was annotated with three to five representative areas, and each slide was then subjected to image segmentation using a template designed to highlight all brown staining, from faint but clearly distinct signals to strong intensities. Immune-positive (brown) immunoreactions were highlighted in red, immune-negative cells and tissue were highlighted in green, and cell-free regions were highlighted in yellow. The immunopositive tissue area fractions in % (red/(red+green) x100) within the chosen annotations were calculated for each case using the same template.

3.4 Statistics

Both the Medcalc Version 20.113 (Ostend, Belgium) program and the R statistical program package (v.4.1.0, R Core Team 2021, Vienna, Austria; RStudio, Boston, MA, United States) were used. While non-normal distribution variables were displayed as the median and interquartile range, categorical variables were tested as proportions. The Cohen's kappa statistics were used to test the pairwise inter-rater agreement of the visual scoring of immunostaining results. [46, 47]. The Spearman's rank test was used to assess the correlations between the experts' scores in pairs at 95% confidence intervals. Using the non-parametric Kruskal-Wallis rank sum test, the discriminating ability of immunoscores among MF-grades created based on Gömöri's silver impregnation was examined. The Wilcoxon-Mann-Whitney U post-hoc test [47] revealed the immunoscores' capacity to distinguish between pairs of MF grades. P values of 0.05 or lower were regarded as significant.

DOI:10.14753/SE.2023.2889

4 RESULTS

4.1 Expression of the growth related markers in non-fibrotic bone marrow

L-NGFR was found in the bodies and processes of elongated, unevenly arranged stromal cells both in peritrabecular and perisinusoidal regions of MF-1 bone marrow samples with sporadic interconnections similar to Gömöri's silver impregnation (*Figure 3* A,B). These regions appeared to be normal and intact. Phosphorylated ERK1-2 was primarily observed in oval cell nuclei and rarely in their processes (*Figure 3* C). CXCL12 positivity was linked to randomly dispersed, elongated cell bodies and scarce processes, and with a weak extracellular reaction (*Figure 3* D).

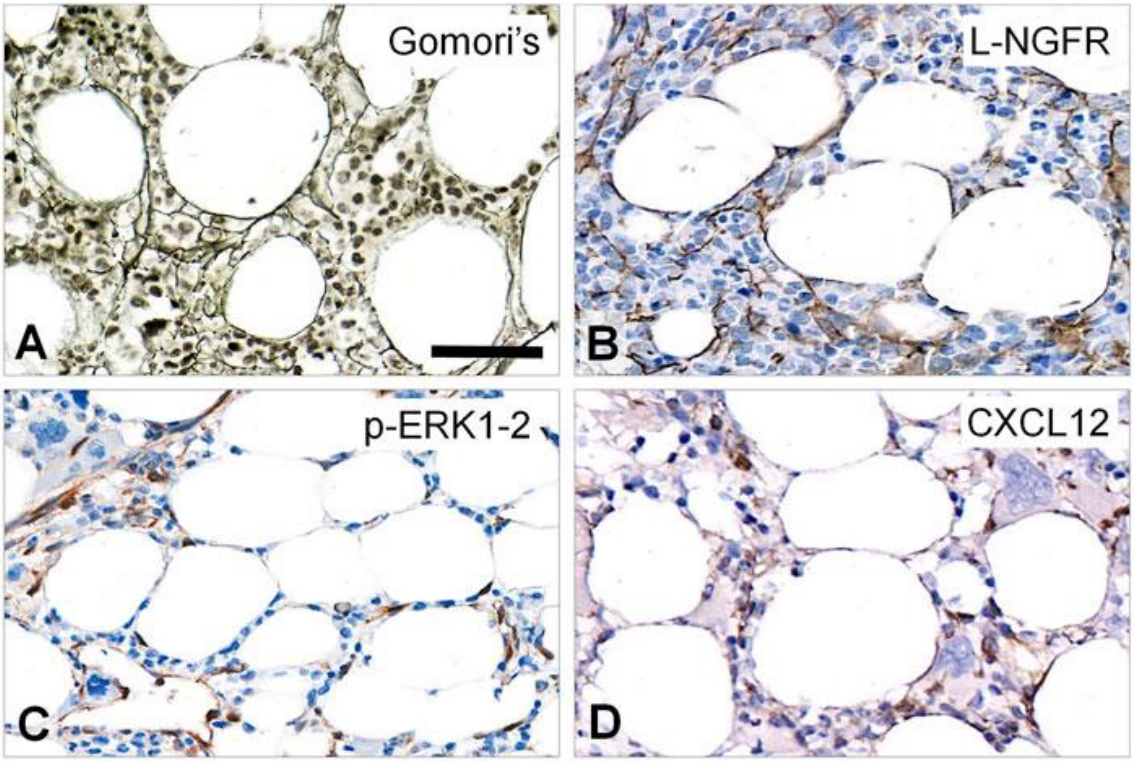

Figure 3. Staining pattern of the tested immunoreactions in intact areas of MF-1 bone marrow samples compared to Gömöri's silver impregnation (A). L-NGFR highlights random stromal cells with their thin processes (B). Phosphorylated ERK1-2 (p-ERK1-2) is detected mainly in oval nuclei of stromal and endothelial cells (C), while the CXCL12 reaction stains the cell bodies of these elements (D) with both revealing only few cell processes. DAB immunoperoxidase reactions (brown) counterstained using hematoxylin (B–D). Scale bar: 50 μm [11].

4.2 Expression of the growth related markers in myelofibrosis

In line with the progressing fibrosis, each and every immunoreaction that was tested demonstrated an increased number of marker-positive cells. L-NGFR staining in perisinusiodal fibroblasts (pericytes) was evident around arterioles, and high power views also confirmed this around capillary sinuses; however, there was no staining of the inner lining endothelial cells in any of the specimens (Figure 4 A). This was the only marker that could only be found in stromal cells, while endothelial cells displayed both p-ERK1-2 and CXCL12 reactions (Figure 4 B,C). Immunopositive cell processes were frequently detected in close association with aberrant megakaryocytes with all three marker reactions (Figure 4D-F), which suggests a close interaction and functional cooperation with them.

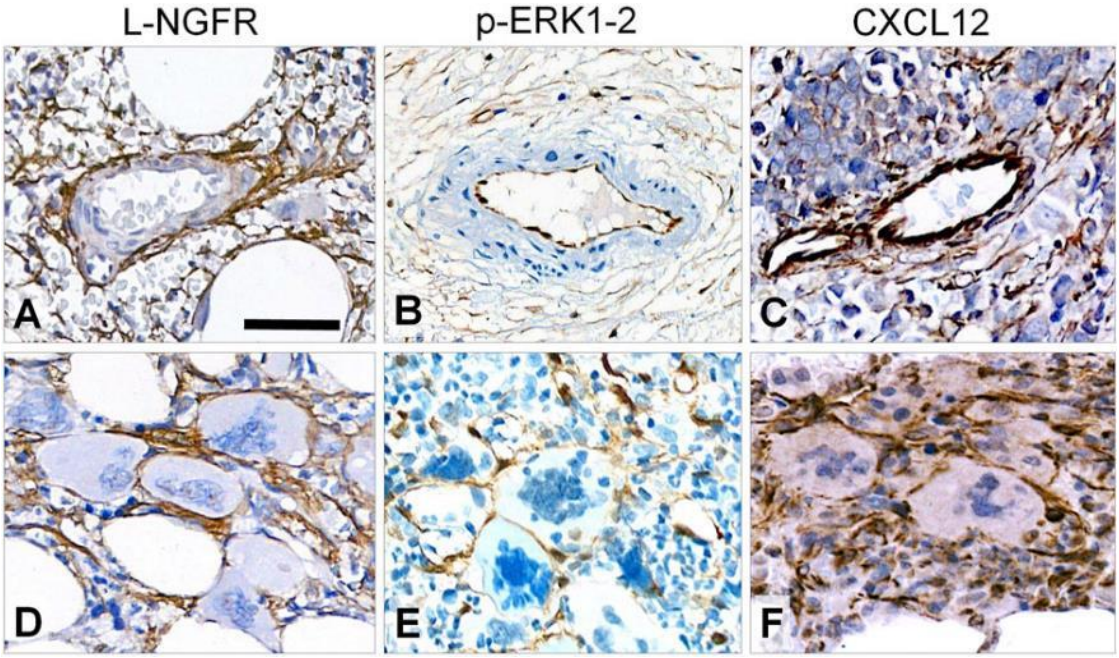

Figure 4. Immunoreaction patterns of the tested markers in arteries, periarterial stroma, and abnormal megakaryocytes in myelofibrosis. L-NGFR positive stromal network spread from adventitial pericytes without endothelial reaction (A); while both p-ERK1-2 (B) and CXCL12 (C) reactions occur in endothelial and inter-arteriolar stromal cells with rare interconnections (upper row). Immunopositive elongated cell processes are intimately associated with aberrant megakaryocytes with all three markers (D, E and F; lower panel). DAB immunoperoxidase reactions (brown) were counterstained using hematoxylin. The scale bar is 100 μm on A and B; and 50 μm on C-F [11].

4.3 Correlations between growth related marker expression and myelofibrosis grade

4.3.1 L-NGFR as the most effective indicator of myelofibrosis grades of the growth related biomarkers

The incidence and density of positive stromal cell bodies and processes for the tested markers at "hot spots" (areas where marker reactions were observed at the highest density) were compared to the Gömöri's-reticulin silver staining based grading using a similar three-tier grade scale (MF-1, MF-2, MF-3).

Immunoreactions that were analyzed using digitally scanned slides were scored independently by three expert assessors (Assessors 1 ,2 and 3) using spreadsheets that were specifically prepared for the purpose. The case order in these spreadsheets has been randomized for each assessor, and the only information that was displayed was the case ID. After having each reaction individually scored during both parts of the study, the assessors met to come to an agreement on a single consolidated score. The comparison and correlation between the immunoreactions of these consolidated scores and the original Gömöri's reticulin silver staining-based grading of myelofibrosis grades established the basis of the study.

When the Kruskall-Wallis rank sum test and the Wilcoxon-Mann-Whitney post-hoc test were applied, the results of the scoring for all three biomarker reactions showed that they were eligible for separation into different grades of myelofibrosis. L-NGFR positive stromal cell density and the scores related to it showed the highest statistical correlations with the Gömöri's' silver staining based fibrosis grades in the results of all three assessors (Figure 5A-C). In addition, a Spearman-rank analysis of the L-NGFR scores demonstrated a strong statistical correlation between the results obtained by the assessors when they were evaluated in pairs (Figure 5D-F).

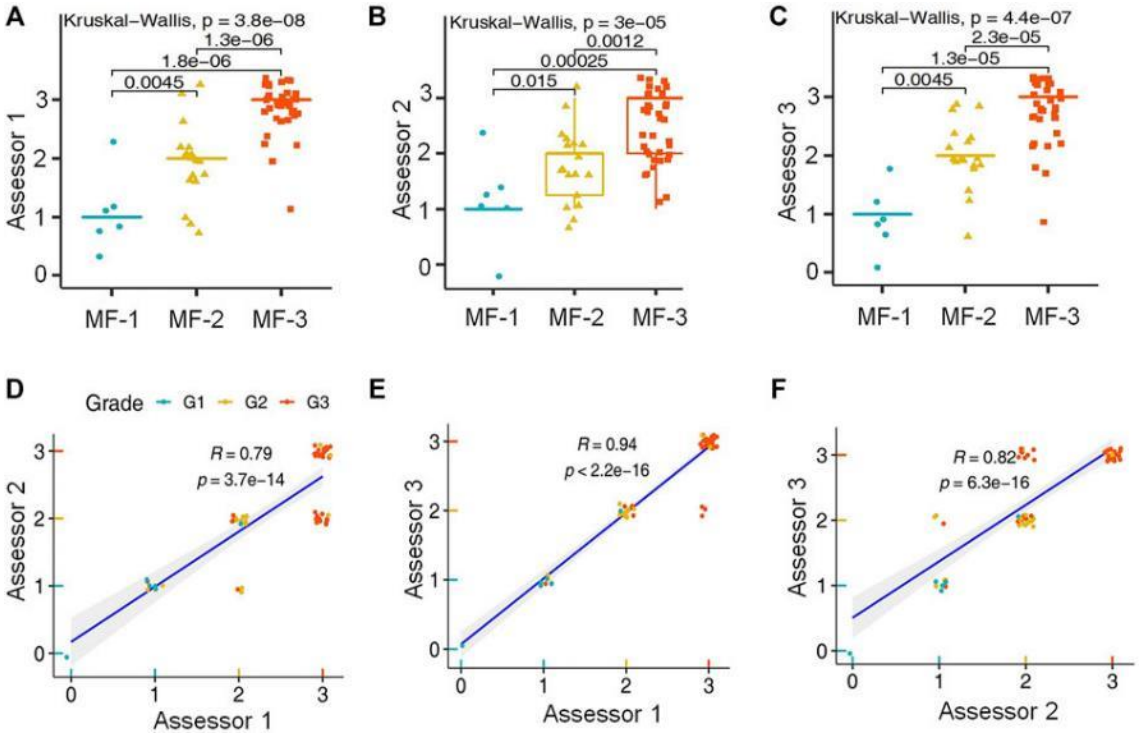

Figure 5. Statistical correlations between L-NGFR immunoreaction scores and Gömöri's silver staining based myelofibrosis grades as recognized by the individual assessors after using both the Kruskal-Wallis test and the Wilcoxon post-hoc test (A–C). Pearson's correlation values among scores of L-NGFR immunoreactions were revealed between pairs of assessors in relation to Gömöri's silver staining based myelofibrosis grades (D–F) [11].

When demonstrated in parallel sections, it was found that the gradually increasing density of L-NGFR positive stromal cell processes (Figure 6A-C) matched with that of the reticular and collagen fibers of silver impregnation (Figure 6D-F). Despite this, it was clear that there were fewer interconnections between L-NGFR positive projections than there were between silver-stained fibers.

When using the Wilcoxon post-hoc test, the consolidated immunoscores that were agreed upon by all assessors produced a result of Kuskall-Wallis p=4.4e-07, along with p=0.0045 between grade 1 and grade 2, p=1.3e-05 between grade 1 and grade 3, and p=2.3e-05 between grade 2 and grade 3 cases (Figure 6G). Cohen's kappa values, which reflect the inter-rater agreement between raters, showed moderate to strong agreement across the cases. The association was found to be moderate between assessors 1 and 2 (kappa =

0.682; z = 7.92; p=1.41e-11); and between assessors 2 and 3 (kappa = 0.664; z = 7.41; p=1.27e-13); however, it was found to be strong between assessors 1 and 3 (kappa = 0.916; z = 9.7; p=0).

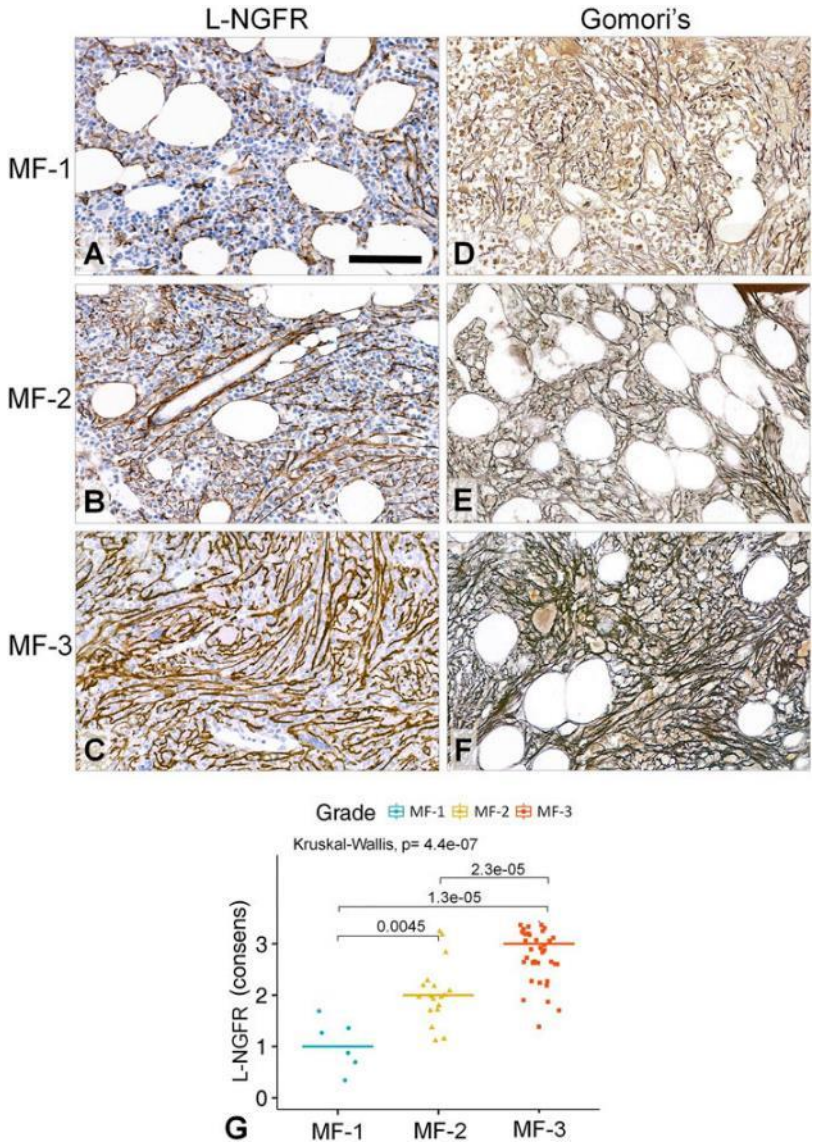

Figure 6. Correlations between the L-NGFR immunopositive stromal network (A–C) and the reticulin (and collagen) scaffolding (D–F) in myelofibrotic bone marrow samples. The gradually increasing density with some interconnections among L-NGFR positive cell processes shows good correlation with reticular (and collagen) fibrosis in determining myelofibrosis grade, as revealed by Gömöri's silver impregnation. DAB immunoperoxidase reactions (brown) were counterstained using hematoxylin (A–C). Scale bar: 50 μm. High statistical correlation was detected between the consensus scores of the three assessors and the sliver impregnation based fibrosis grades both with the Kruskal-Wallis global trend test and the pairwise Wilcoxon post-hoc test (G) [11].

4.3.2 Correlation between the levels of pERK and CXCL12 and the grade of myelofibrosis

When compared to the value of L-NGFR, the consolidated scores of both p-ERK1-2 and CXCL12 demonstrated a significance that was less prominent concerning their grade separation values. These markers were primarily found in the nuclei (p-ERK1-2) and in the cytoplasm (both p-ERK1-2 and CXCL12) of stromal cells, which projected only thin processes and had almost no interconnections between them (Figure 7A-D). When using the Wilcoxon post-hoc test, the consolidated immunoscores for p-ERK1-2 resulted in a p value of 0.00039 for the Kuskall-Wallis test, in addition to p values of 0.015 between MF-1 and MF-2, p values of 0.0063 between MF-1 and MF-3, and p values of 0.014 between MF-2 and MF-3 for cases. For CXCL12, the consolidated immunoscores led to a Kruskall-Wallis p value of 3.3e-05, followed by Wilcoxon post-hoc test values of p = 0.0098 between grade 1 and grade 2, p = 0.00016 between grade 1 and grade 3, and p = 0.0021 between MF-2 and grade MF-3 cases. Both p-ERK1-2 and CXCL12 immunoreactions were less evident for straight assessment, which was also reflected by their weaker Spearman-rank correlations (pERK1-2, R=0.76-0.81; CXCL12 R=0.82-0.89) and Cohen's kappa interrater values only having weak correlations (*p*-ERK-1-2, kappa = 0.415–0.526; CXCL12, kappa = 0.512–0.578) than those of L-NGFR.

DOI:10.14753/SE.2023.2889

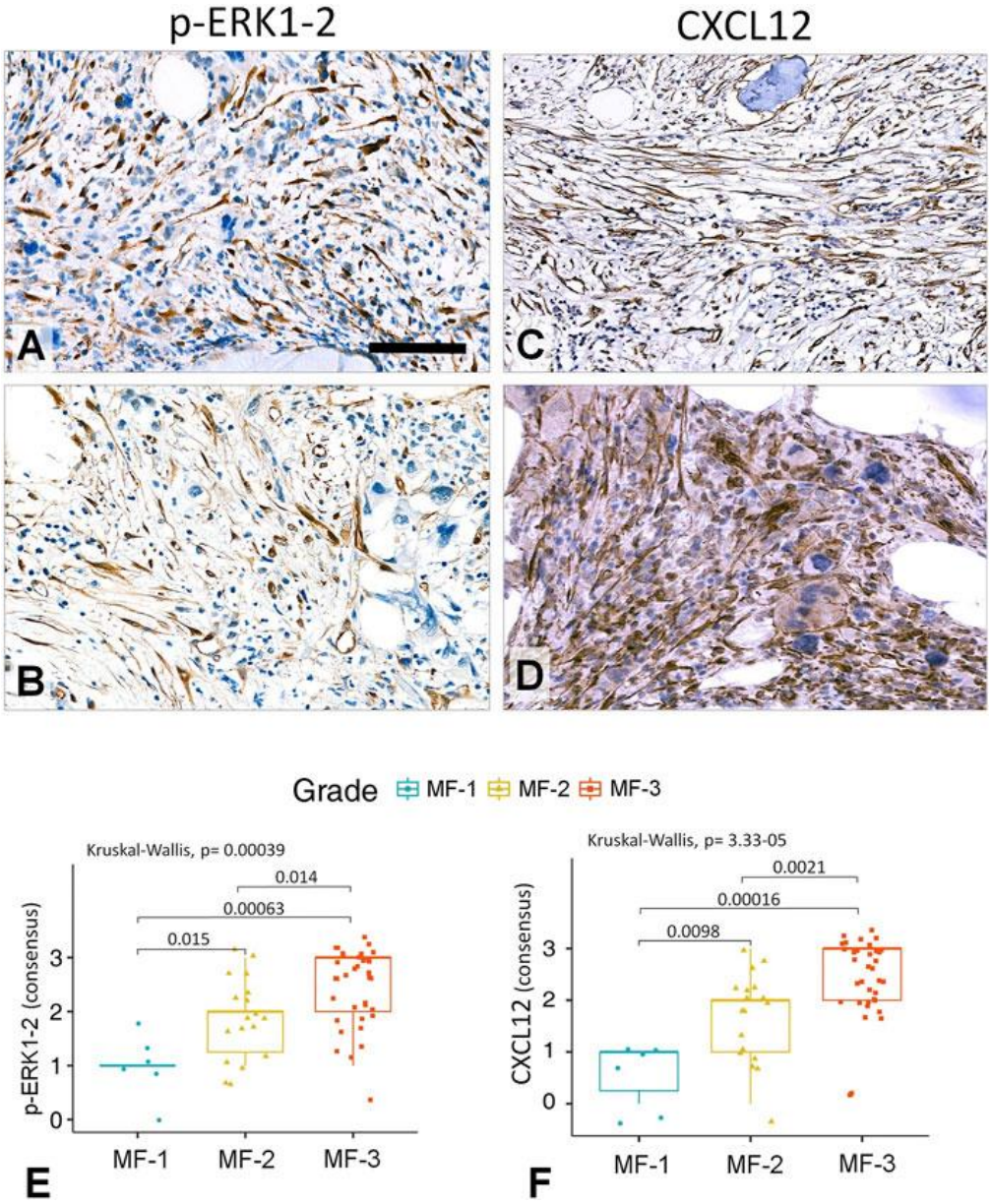

Figure 7. Representative examples of grade 3 myelofibrotic bone marrow samples where either p-ERK1-2 (A, B) or CXCL12 (C, D) immunoreactions reveal elongated stromal cells, which are however, are rarely interconnected by their processes into contiguous meshworks. DAB immunoperoxidase reactions (brown) counterstained using hematoxylin. The scale bar is 50 µm on A, B and D; and 100 µm on C. Both the p-ERK1-2 (E) and CXCL12 (F) immunoreaction consensus scores showed statistical correlations with reticulin-silver staining based myelofibrosis grades, either when using the Kruskal-Wallis trend test or the pairwise Wilcoxon test. However, their discrimination power was weaker than that of L-NGFR [11].

4.3.3 L-NGFR-positive stromal network was found to be colocalized with connexin 43 gap junction plaques

Previously, we found that the Cx43 direct cell-cell communication channels were upregulated in pathological bone marrow samples [27]. These samples had a higher ratio of stromal cells to hemopoietic cells. Therefore, L-NGFR, which was found to be the most effective marker in this study for highlighting the stromal network, and Cx43 protein were analyzed simultaneously using immunofluorescence in samples representing all grades of myelofibrosis in order to investigate the possibility of a link between the two (Figure 6A-C). The results of multilayer scanning showed the presence of Cx43-positive particles with a size of 1 μm throughout the 4 μm section thickness, as well as a significant co-localization between these particles and L-NGFR-positive stromal cell processes. After highlighting the specific reactions in each channel through image segmentation, the HistoQuant software was utilized for the purpose of quantitatively analyzing both reactions in representative areas (67 areas and 10 cases) (Figure 8D-E). After combining the various immune signals in segments, the massive co-expression of the two biomarker reactions became immediately apparent (Figure 8D). The Spearman rank correlation test was utilized in order to analyze the degree of association between the two different makers' expressions, which revealed significant statistical correlations (Figure 8E).

DOI:10.14753/SE.2023.2889

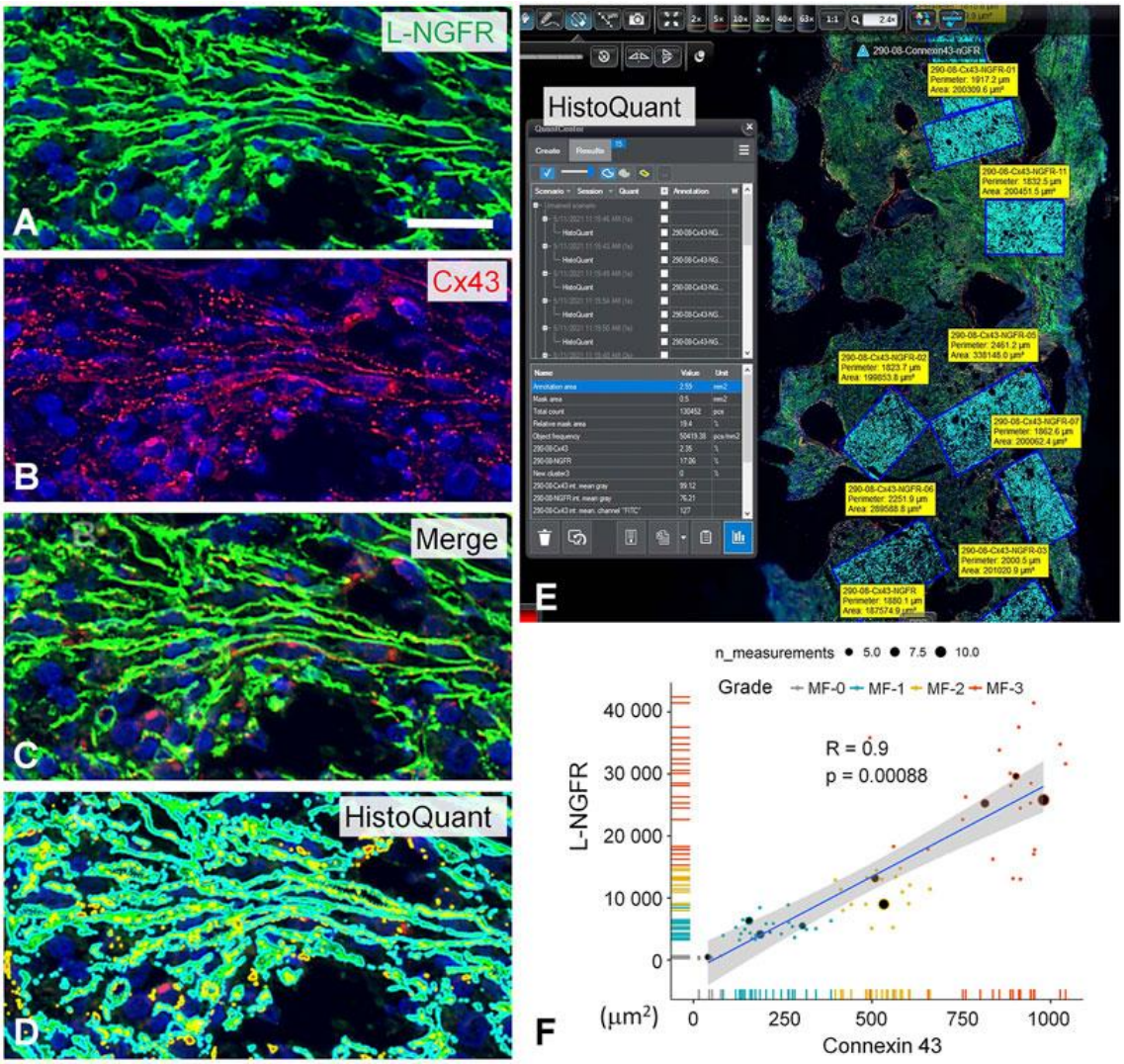

Figure 8. Double immunofluorescence for L-NGFR (green, A) and Cx43 (red, B) along with Hoechst nuclear counterstain (blue) in a grade 3 myelofibrosis. Merged images proved massive colocalization of the biomarkers (C), which became apparent after highlighting the green (in turquoise) and red signals (merged in yellow) with the image segmentation algorithm of the HistoQuant software (D). Semiautomated image analysis of the area fractions of fluorescent signals with this program in 67 standard areas of 10 myelofibrotic marrow samples (E) revealed strong overlap and correlation between L-NGFR and Cx43 signals, suggesting that most particulate Cx43 belongs to L-NGFR positive stromal cells (F). The scale bar on A is 25 µm on A-D and 500 µm on E [27].

4.4 Expression of extracellular matrix proteins in non-fibrotic bone marrow

Positive results for type I and type III collagens were seen in randomly dispersed fragmented fibrillary structures in all normal and five pre-fibrotic cases (Figure 9A-B).

The fibrillin-1 reaction was the most striking response to highlight a continuous matrix network supporting blood vessels and defining adipocyte membranes. (Figure 9C). Only one of the five bone marrows with normal morphology was given a score of MF-1 based on the reactions evaluated by type I collagen (by two assessors) and type III collagen (by one expert). But this case, along with all of the other normal and pre-fibrotic cases, was finally agreed to be MF-0 with any of the other markers.

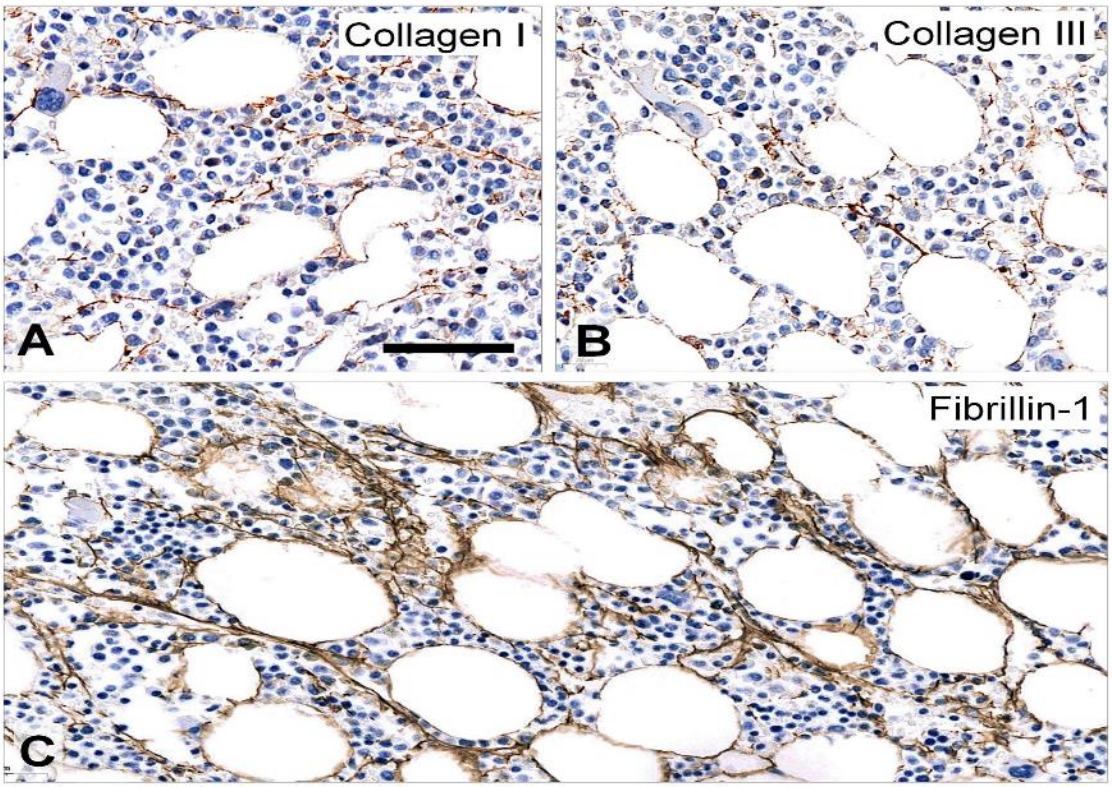

Figure 9. Immunoperoxidase staining (brown) in serial sections of a prefibrotic bone marrow revealed only fragmented Type-I (A) and type-III (B) collagen fibers, while the fibrillin-1 (C) reaction highlighted a more continuous matrix network supporting blood vessels and delineating adipocyte membranes. Scale bar: 80 um [48].

4.5 Expression of extracellular matrix proteins in fibrotic bone marrow

In myelofibrosis, all three immunoreactions highlighted the activated stromal cells and matrix scaffolding of bone marrow samples in similar patterns and densities to the reticulin (and collagen) structures revealed by Gömöri's silver impregnation. Generally speaking, these similarities were in line with the severity of the disease. Based on

immunoreactions against type I collagen and fibrillin-1, a few cases were moved up from the MF-2 category to the MF-3 category (Figure 10). On the other hand, downgrading was also seen. For fibrillin-1, the proportion of cases that were upgraded or downgraded by one grade was 6/7, while for type I collagen it was 5/9 and for type III collagen it was 4/17. In general, type III collagen immune-positive fibrils were always smaller and less intense compared to those revealed by type I collagen and fibrillin-1 reactions. This was the case regardless of the size or length of the fibrillum [48].

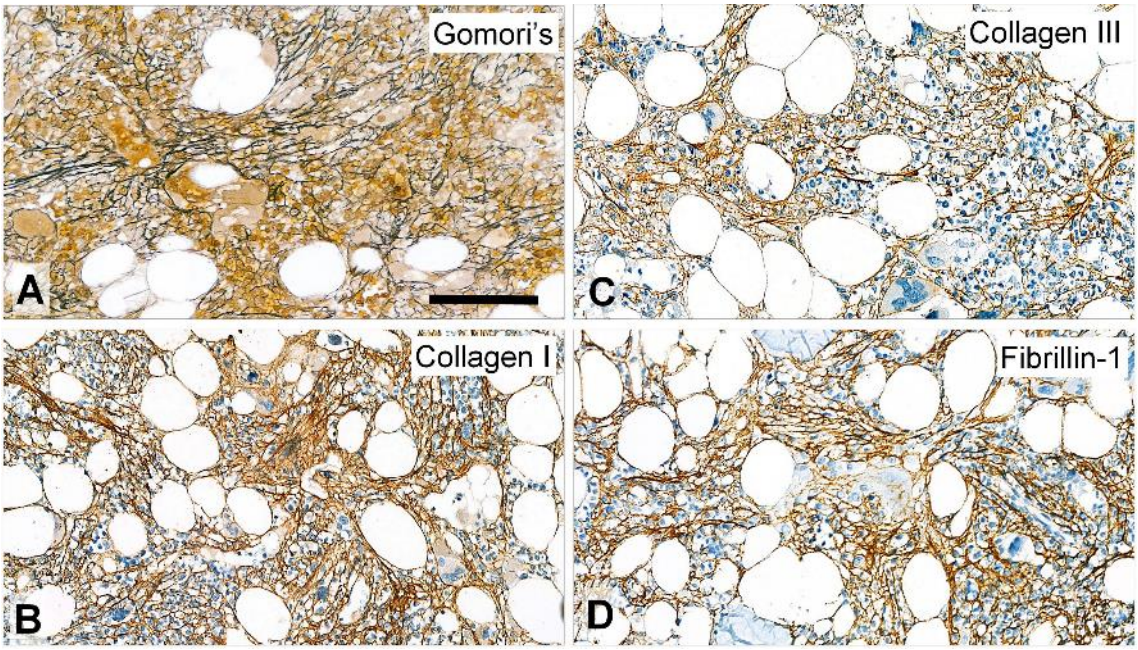

Figure 10. Serial sections of a myelofibrotic bone marrow were considered grade 2 (MF-2) based on Gömöri's silver impregnation (A) and also scored as such after type III collagen immunoreaction (B), but scored for grade 3 (MF-3) after type I collagen (C) and fibrillin-1 (D) reactions. Scale bar: 150 µm [48].

Immunostaining with antibodies directed against type I collagen also highlighted bone trabecules, including newly formed bone in osteosclerosis (Figure 11A). However, insufficient preanalytics and bone damage in a few cases caused type I collagen to appear in the adjacent megakaryocytes in a non-specific manner, and these areas were neglected when scoring (Figure 11A insert). The fibrillin-1 reactions that were uniformly strong offered the best visualization of the structural abnormalities of the stromal scaffolding. All of the matrix protein immunoreactions that were tested showed close visual and

statistical correlations with Gömöri's silver staining in patients with advanced MF-3 myelofibrosis (Figure 11B-E).

4.6 Statistical correlations between matrix protein immunoreactions and Gömöri's silver grades

First, the immunoreactions were graded by three separate assessors using criteria that were identical to those used by Gömöri's silver impregnation-based myelofibrosis grading. Just like it was applied in the first part of the study, the scoring spreadsheets have been randomized for each assessor, and the only information that was displayed was the case ID. After having each reaction individually scored, the assessors met to come to an agreement on a single consolidated score in each set. The correlation between each immunoreaction (consolidated scores) and the original Gömöri's silver staining based grading of myelofibrosis established the comparison basis of the study.

Spearman's rank test of the pairwise correlations between the assessors' scores showed the highest rho-values between 0.908-937 for fibrillin-1, 0.866-0.930 for type I collagen, and 0.857-0.915 for type III collagen at p0.0001 significances for all three markers. Fibrillin-1 had the highest rho-values, followed by type I collagen, and type III collagen (Figure 9F-H). Inter-rater agreement between pairs of assessors' scores was tested using Cohen's kappa statistics, which resulted in moderate to substantial agreements for fibrillin-1 (kappa = 0.721-0.847) and type I collagen (kappa = 0.668-0.840), and moderate agreements for type III collagen (kappa =0.593-0.690). Moderate agreements were found for fibrillin-3 (kappa = 0.593-0.690). (Figure 11F-H).

When using the Kruskal-Wallis nonparametric rank test, all of the evaluators found that the density and intensity of immunoreactions and the original MF silver grades were highly significant for all three immune markers. The magnitudes of significance levels with the Kruskal-Wallis test did not change when individual scores were consolidated and agreed on by all evaluators, resulting in p = 2.774e09 for type I collagen; p = 1.159e08 for type III collagen; and p = 2.084e09 for fibrillin-1. The Wilcoxon-Mann-Whitney post-hoc test showed significant statistical differences between MF grades for all three matrix reactions, with the exception of type III collagen between pre-fibrotic and MF-1 and between MF-1 and MF-2. These pairwise statistical differences were found to be high.

The immunoscores of the tested matrix proteins were used to generate detailed significance levels between the MF grades. These levels are summarized in graphs (Figure 9F-H).

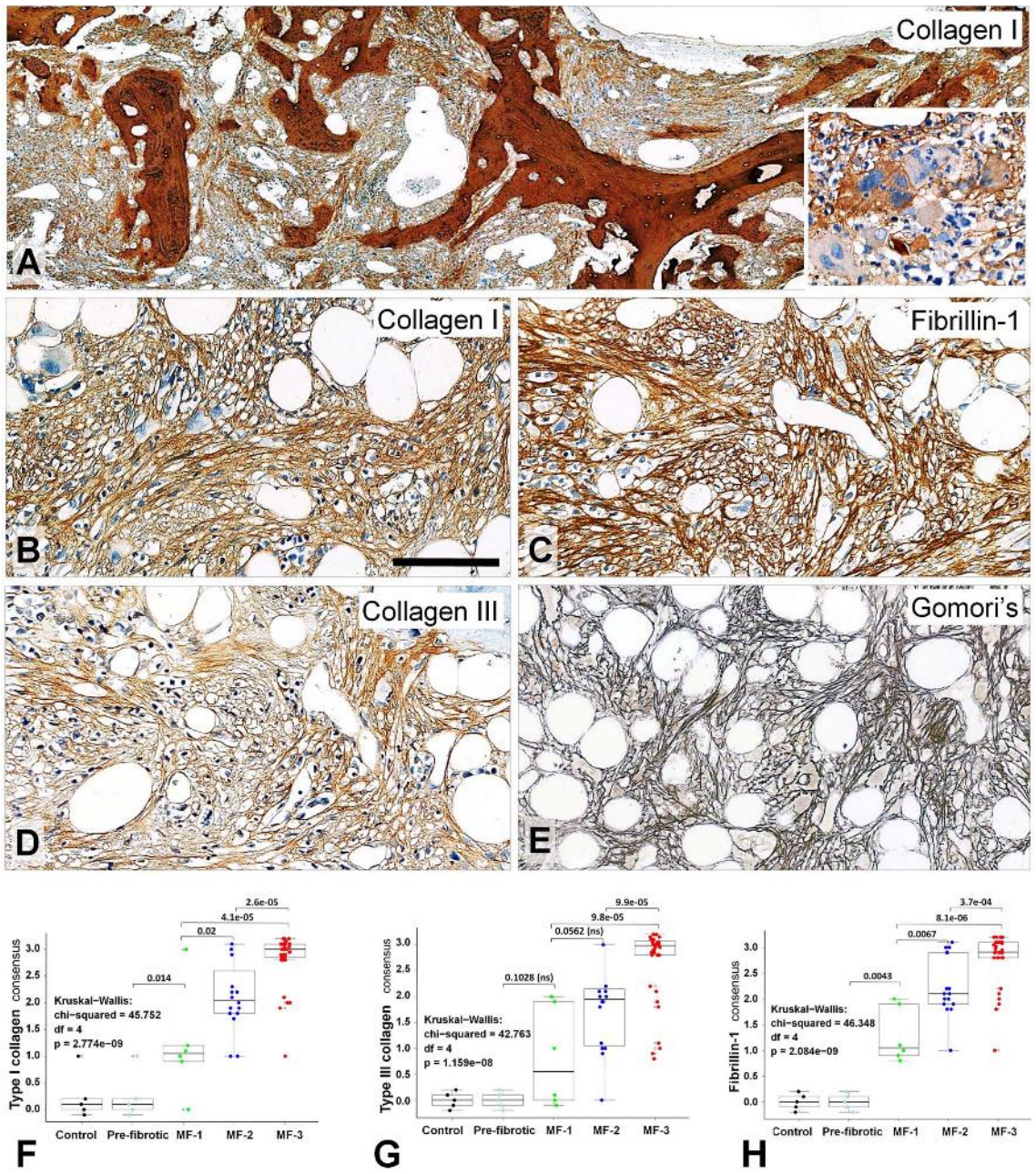

Figure 11. The performance of the tested immunoreactions for Type-I (A-B) and type-III (C) collagens, and fibrillin-1 (D) compared to Gömöri's silver impregnation (E) in advanced (end-stage) grade 3 (MF-3) myelofibrosis. Type I collagen immunoreaction revealed bone trabeculae and osteosclerosis, besides myelofibrosis (A) and occasionally was flown into adjacent megakaryocytes (inset). Higher power shows immune positive stromal cells and dense fibrillary arrays projecting out from them for both type I collagen

(B) and fibrillin-1 (C) reactions, as well as type III collagen as more delicate fibrils (D) all in a similar pattern to silver staining (E). Scale bar on B represents: 500 μm on A and 100 μm on the inset; and: 150 μm on B-E. Graphs demonstrate the statistical correlations between type I (F) and type III collagen (G) and fibrillin-1 (H) immunoreaction scores after consolidation and the Gömöri's silver impregnation based myelofibrosis grades using both the Kruskal-Wallis test and the Wilcoxon post-hoc test [48].

4.7 The expression of matrix proteins reveals further characteristics in myelofibrosis

Strong and dense immunostaining was observed for type I and type III collagens in fibrillary arrays of periarteriolar fibroblasts (pericytes) and matrix anchoring the external elastic lamina of the tunica adventitia. However, relatively sparse staining was observed for fibrillin-1 (Figure 12 A-B-C). On the other hand, the folded internal elastic lamina of arterioles stained only for fibrillin-1, while arterial smooth muscle cells in the media displayed all three reactions randomly. In the cell-rich areas of MF-3 cases, groups of atypical megakaryocytes were found to be enveloped by the immunopositive fibrillary matrix with all 3 reactions, whereas the distal areas predominately displayed type I collagen and fibrillin-1 matrix (Figure 12 D-E-F). In osteosclerosis, the bone itself as well as the bone-forming osteoblasts were highly immunopositive for type I collagen.

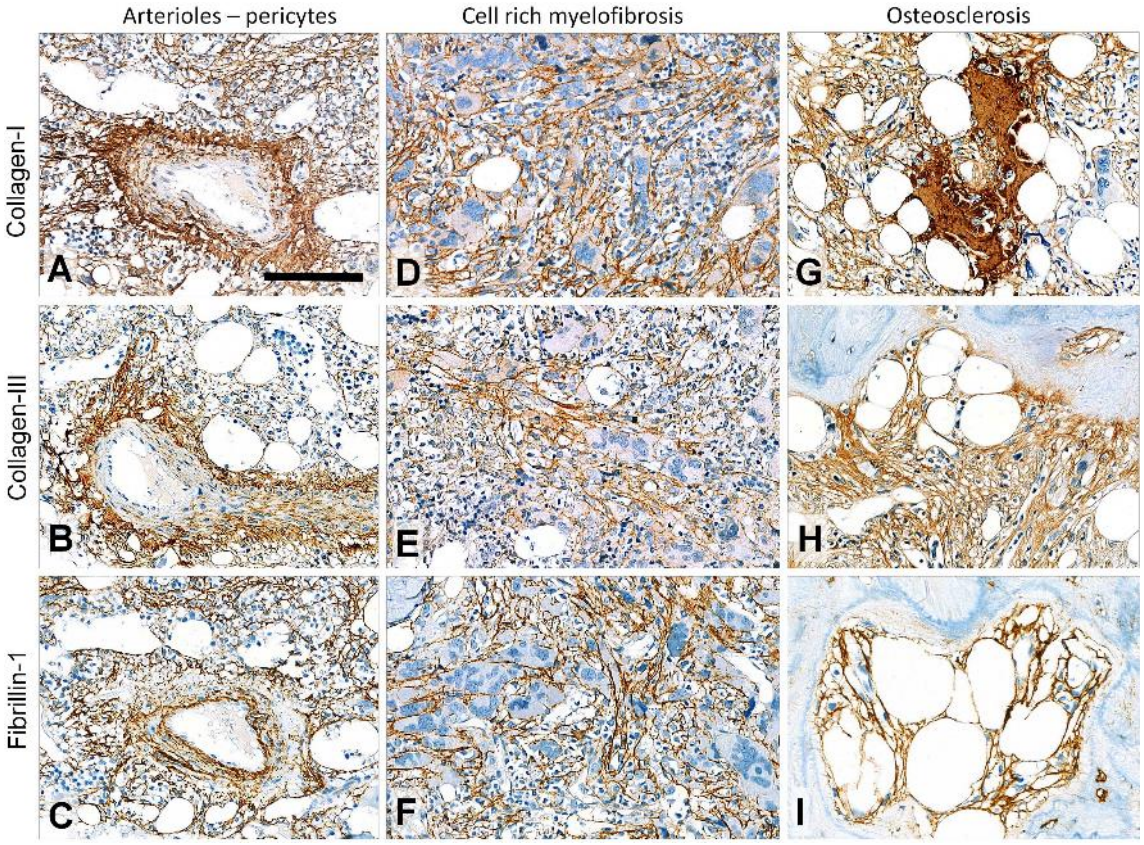

Figure 12. Characteristic staining patterns of type I and type III collagen, and fibrillin-1 immunoreactions in advanced MF-3 myelofibrosis. Serial sections of an arteriole (left column) show dense reactions of pericytes and adjacent matrix for type I (A) and type III (B) collagens; and only occasional reactions at this location but obvious staining of the elastic lamina interna for fibrillin-1 (C). The fragmented staining among vascular smooth muscle cells was less intense for type III collagen. In a cell rich myelofibrosis (D-F) all 3 reactions stained the fibrillar matrix among atypical megakaryocytes, but the type III collagen reaction gradually diminished distally from these locations (E). In osteosclerosis, the actively bone forming osteoblasts and the bone were strongly positive for type I collagen (G), while type III collagen (H) and fibrillin-1 (I) reactions stained an endosteal rim only with an additional fibrillin-1 reaction in osteocytes. Newly formed bone is seen between the blue rim and the endosteal collagen III and fibrillin-1 immunoreactions. Scale bar: 150 μm [48].

Osteocytes expressed fibrillin-1, and type III collagen and fibrillin-1 reactions formed rims at the endosteal bone marrow margin without active osteoblasts (Figure 12 G-H-I). Even though the number and size of capillary sinuses were growing in several advanced MF-3 cases, mature red blood cells infiltrated the remnants of stromal scaffolding without

endothelial lining, as shown by all three immunoreactions. This was the case despite the fact that capillary sinuses were increasing (Figure 13).

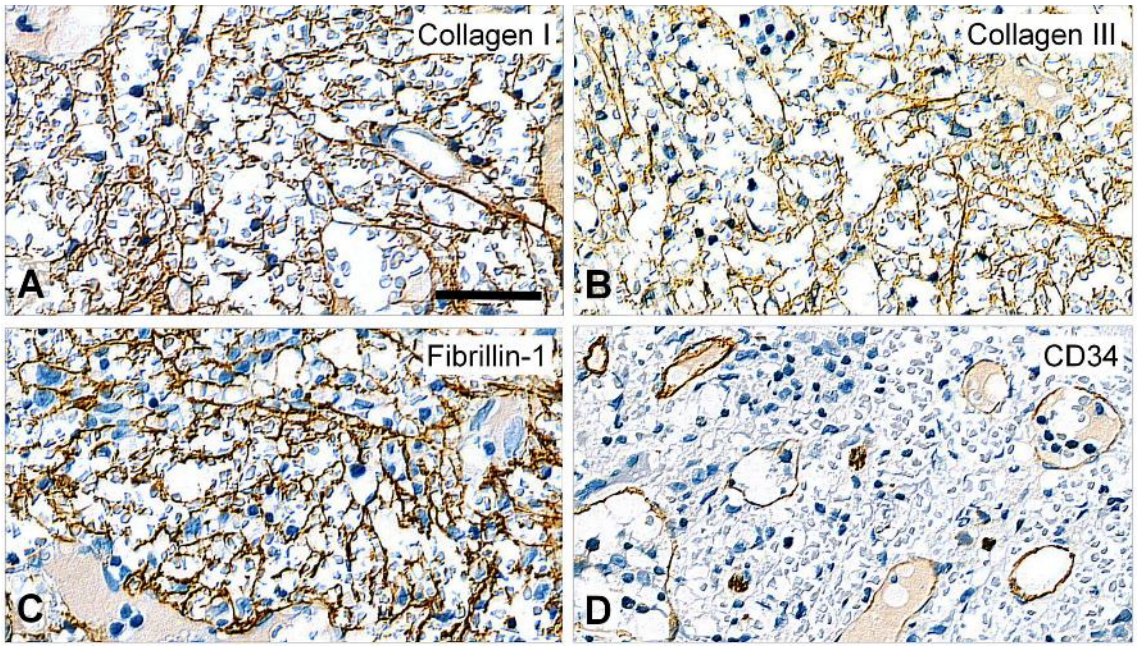

Figure 13. Remnants of stromal scaffolding revealed by all 3 immunoreactions tested for type I (A) and type III (B) collagens and fibrillin-1 (C) with heavy infiltration by red blood cells without endothelial lining (D) in serial sections of an advanced MF-3 myelosibrosis. Type III collagen reaction (B) highlights the finest fibrillar structures. Digital differential interference images. Scale bar: 80 μm [48].

4.8 Myelofibrosis grade determined through computerized image analysis of fibrillin-1 immunoreactions

According to the statistical results and the findings of the visual scoring, the fibrillin-1 reaction proved to be the one that would be best suited for automated whole slide image analysis. Using the same adjustment setup template for digital image analysis different colors (red, green and yellow) were used for training the recognition algorithm of image analysis (Quant Center, PatternQuant modul) (Figure 14).

DOI:10.14753/SE.2023.2889

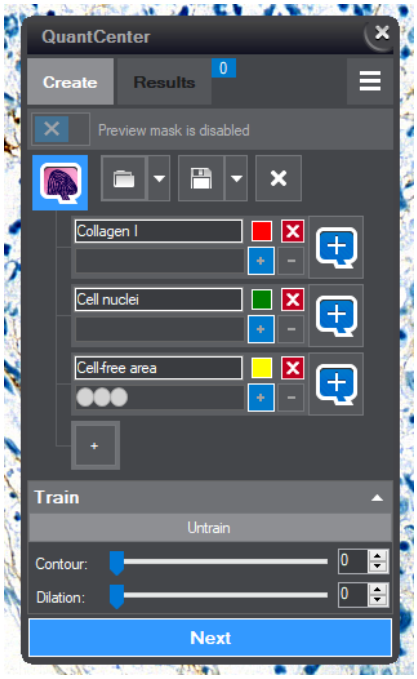

Figure 14. Quant Center (3Dhistech Ltd.), modul for PatternQuant setup. Based on color ranges and pattern characteristics, distinct colors (red, green, and yellow) were used to highlight and distinguish different areas in the digital image.

Beside the brown colored immunoreaction, the additional negative tissue, the cell-free areas, and cell nuclei were automatically highlighted with different colors (Figure 15A-D). The myelofibrosis grades that were determined by Gömöri's silver impregnation overlapped with the fibrillin-1 positive area fractions that were found within the bone marrow tissues. The Kruskal-Wallis rank sum test showed that there is a highly significant statistical difference between MF-grades based on the image analysis results (Figure 15E-F), which is comparable to the results obtained through eye control scoring (Figure 15E). The discriminating power of fibrillin-1 immunoreaction quant results between pairs of MF grades was also validated by the Mann-Whitney U post-hoc test. In the image analysis graphs, the 7 cases that were visually upgraded and the 6 cases that were visually downgraded compared to the original MF grades appeared in the upper and lower regions, respectively. (Figure 15E).

DOI:10.14753/SE.2023.2889

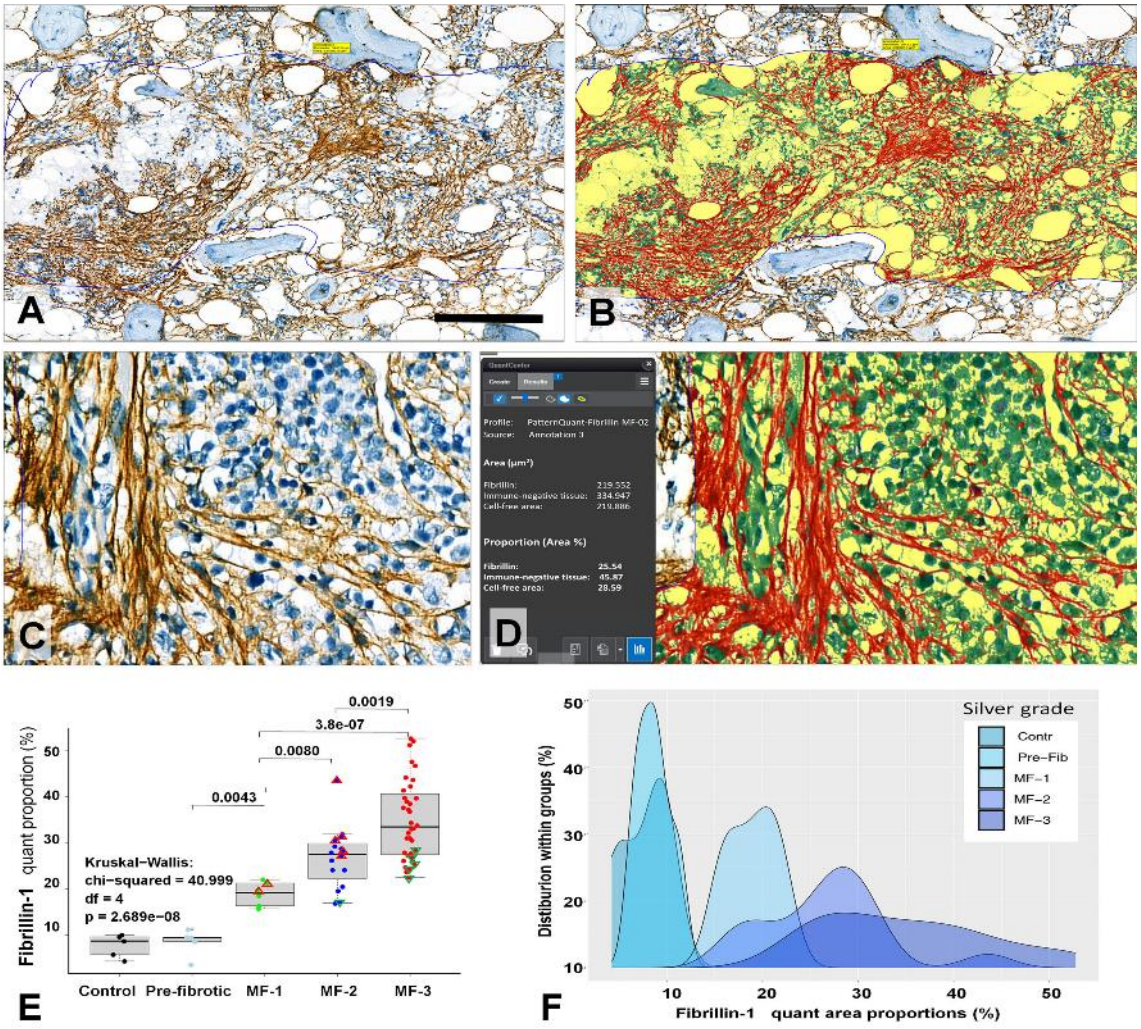

Figure 15. Automated image analysis using the PatternQuant machine learning algorithm for measuring the proportions of fibrillin-1 immunoreaction (A and C, brown) within representative annotated areas of myelofibrotic bone marrow sections. Image segmentation reveals areas occupied by the immunoreactions (red), the immune-negative tissue (green) and the cell-free regions (yellow) (B and D). Higher power confirms the accuracy of segmentation (B and D). The highlighted numbers in D show measured areas in µm2 and in % proportions. The scale bar represents 300 µm on A and B; and 50 µm on B and D. Graphs demonstrate the statistical correlations between fibrillin-1 quant analyzed and the Gömöri's silver impregnation based myelofibrosis grades using both the Kruskal-Wallis test and the Wilcoxon post-hoc test (E). The 7 cases that were upgraded (red triangles) and 6 cases that were downgraded (green triangles) at the visual scoring were segregated to the upper and lower regions, respectively, within their MF categories in the boxplots. The overlapped distribution of quant results within MF-grades (F) confirms the continuous nature of myelofibrosis progression [48].

5 DISCUSSION

Bone marrow fibrosis, which is a consequence of abnormal activation of the fibrogenic stromal microenvironment, is still a major predictor of the outcome in primary myelofibrosis [39, 49]. This is true despite the fact that novel prognostic models have been developed that take into account driver and passenger mutations, karyotypes, and sex-adjusted hemoglobin levels. In our study, we tested growth related markers that were primarily expressed by stromal cells. These markers included L-NGFR/CD271, p-ERK1-2, and CXCL-12. We discovered that the density of positive cells for each marker increased in a manner that was consistent with the Gömöri's silver staining-based tumor grade levels. NGFR reactions that were restricted to and labeled the entire length of stromal cells showed the strongest statistical correlation and the most reproducible agreement among assessors' judgments regarding immunoreaction based myelofibrosis grades. Specifically, in advanced myelofibrosis, L-NGFR positive stromal cells were found to co-express the Cx43 protein, which suggests increased communication and functional coupling within the overgrown stromal network. As a result, our research revealed a few biomarkers of stromal cell activation, the most promising of which was L-NGFR expression as a supplement to Gömöri's silver staining for myelofibrosis grading.

Myelofibrosis is driven by an increased and pathological production of extracellular matrix. This is caused by an increase in the number of activated bone marrow stromal cells as a result of abnormal cytokine signaling and clonal megakaryocyte functions. This, in turn, is caused by an increase in the number of bone marrow stromal cells [50]. Primary myelofibrosis grades are determined by the extent of matrix overproduction, which is still evaluated using Gömöri's silver impregnation. The extent of matrix overproduction also predicts disease progression and outcome [49]. On the other hand, selective silver deposition on reticular and collagen fibers can be highly dependent on preanalytical (fixation, decalcification) and staining (components, timing, ambient temperature, and light conditions) variables [39,51]. Even though none of our chosen growth-related markers highlighted the reticular or collagen matrix in the bone marrow, these markers were predominantly expressed in stromal cells and were linked to growth-related pathways as potential indicators of their activation. An intimate association of spindle-shaped stromal cells, which were positive for each marker, with aberrant megakaryocytes was likely to

reflect their functional cooperation and the potential impact of cytokines and growth factors released by megakaryocytes on pathological stromal cell activation. This was likely due to the fact that spindle-shaped stromal cells were positive for each marker.

L-NGFR (CD271) is a low affinity receptor for neurotrophins, including NGF. It is able to catalyze its receptor tyrosine kinase (RTK) mediated signaling in neurons by cooperating with tropomyosin receptor kinase A (TrkA) [52, 53]. Alternately, L-NGFR may prevent this growth signaling, which may lead to a programmed cell death response (apoptosis), for example in oligodendrocytes [54]. This may occur when L-NGFR interacts with non-preferred neurotrophins. According to the results of our research, L-NGFR expression increased over time in the expanding stromal cell network that promotes the progression of the disease in myelofibrosis. This finding points to its involvement in growth promotion rather than apoptosis. Despite the fact that Trk neurotrophin receptors have only rarely been detected in the bone marrow stromal network [55], it is possible that TrkA will be of assistance to L-NGFR in this regard. Both of these proteins are thought to be involved in the functions of mesenchymal stromal cells [56]. In spite of this, the finding that upregulated TrkA in bone marrow stromal stem cells can augment their survival and regenerative capacity in nerve grafts by way of the MAPK pathway can also support this view [19]. It's possible that stromal cells in the bone marrow could also produce nerve growth factor, which brings up the possibility of autocrine regulation of stromal proliferation [57]. L-NGFR expression was first seen in bone marrow stromal cells almost 30 years ago, at a time when its correlation with reticulin silver staining in myelofibrosis was already mentioned. However, this correlation was only based on two cases at the time [14]. Immune electron microscopy of L-NFGR confirmed the presence of labeling all along the stellate or spindle-shaped filamentous stromal processes, most prominently in bone marrow adventitial reticular cells [58]. This lends credence to our observation that the L-NGFR immunoreaction was present along the entire length of the stromal cell processes in the myelofibrotic bone marrow. L-NGFR/CD271 has been considered as selective marker for the isolation of mesenchymal stromal (stem) cells. This is due to the fact that positive cell fractions contain a high number of clonogenic precursors, which exhibit increased proliferation [59] and trilineage differentiation into fibroblastic, adipocytotic, and osteoblastic cells, significantly more than CD271 negative stromal cells [17, 60]. These findings also imply that L-NGFR/CD271 plays a role in the functional activation of the

stromal network in bone marrow. L-NGFR immunoreaction was recommended for differential diagnosis within myeloproliferative neoplasms after it was shown that positive stromal cells were more frequent in primary myelofibrosis than in essential thrombocytosis (ET) or in polycythaemia vera (PV) [61]. However, its correlations with myelofibrosis grades had not been studied systematically prior to this study. Both the Kruskall-Wallis global trend-tests and the Wilcoxon post-hoc test demonstrated that the L-NGFR reaction exhibited the highest discriminating power of the biomarkers that were tested in our research. This was the case regardless of the myelofibrosis grade. This was the only marker that could be identified solely in stromal cells and in all of their processes. Furthermore, L-NGFR scores demonstrated the best interrater agreement between pairs of assessors; consequently, the L-NGFR immunoreaction can be a biological indicator of stromal cell activation and overproduction of reticular and collagen fibers, as revealed by silver impregnation. This was demonstrated by the fact that L-NGFR scores demonstrated the best inter-rater agreement between pairs of assessors.

The signaling of receptor tyrosine kinase (RTK) is the primary factor in the promotion of profibrogenic responses [62]. RTKs, and possibly TrkA as well, have been found to play a significant role in the regulation of mesenchymal stromal cell activation, growth, and proliferation, which includes the bone marrow stromal microenvironment. This is accomplished primarily via PDGFR, EGFR [63], and FGF2/bFGF receptors [64]. PDGFR-beta expression, (but not PDGFR-alfa), was found to indicate the functional activation of bone stromal cells in the myelofibrotic marrow and to statistically correlate with the Gömöri's silver impregnation based fibrosis grades [21-23.] This was found to be the case despite the fact that PDGFR-beta expression was also found to indicate the functional activation of bone stromal cells in the normal marrow. RTK signaling converges on ERK1-2 phosphorylation as a sign of its activation. This results in p-ERK1-2's translocation into the cell nucleus, where it acts as a transcription factor to promote growth and proliferation related adaptation responses in stromal fibroblasts [65, 66]. Our p-ERK1-2 immunoreactions, which occurred both in the nuclei and the cytoplasm of spindle-shaped cells, provide evidence that this is the case. However, the reaction did not highlight the entire length of the stromal cell processes, and as a result, it rarely showed any interconnections. Additionally, the reaction occurred in some sinus endothelial cells that had a similar morphology. In spite of these limitations, p-ERK1-2 protein positive

cell density was found to have a statistical correlation with the progression of myelofibrosis, which was consistent with Gömöri's silver impregnation. Although the p-ERK1-2 immunoreaction was shown to be another biomarker of bone marrow stromal cell activation and the progression of myelofibrosis, it demonstrated a lower potential for diagnostic application in comparison to the NGFR reaction.

The chemokine CXCL12 is constitutively released from bone marrow stromal cells. It plays a role in the maintenance of stem cells in bone marrow niches by binding to CXCR4 on CD34+/CD117+ hemopoietic progenitors and leukemic blasts [24], respectively. CXCR4 is downregulated in malignant progenitors, which may explain extramedullary clonal hematopoiesis in myelofibrosis [67]. As a result, CXCL12 may also play a role in protecting leukemic stem cells and contributing to the progression of myelofibrosis [30]. Endothelial cells have the potential to express CXCL12, albeit at a lower level than other cell types. CXCL12 is an essential component in the process of stem cell homing during transplantation, and the interaction between CXCL12 and CXCR4 helps to support stromal cell resistance and the restoration of the stromal network after myeloablative irradiation [25]. Oncogenic *JAK2*, which frequently suffers activating mutations in primary myelofibrosis [28], is responsible for initiating the CXCL12/CXCR4 pathway's activation. In line with this, we found CXCL12 positive perivascular and periosteoblastic stromal cells at increasing densities with increasing grades of myelofibrosis based on Gömöri's silver staining. However, similar to the situation with p-ERK1-2, CXCL12 immunoreactions may not reveal all of the stromal cells and may only highlight a portion of the stromal cell bodies. The fact that the mild extracellular staining was consistent with CXCL12 functions, on the other hand, was another factor that prevented it from being a useful diagnostic biomarker of the progression of myelofibrosis.

Connexins are responsible for the formation of direct cell-cell communication channels, which enable the controlled passage of small regulatory molecules (less than 1.8 kilodaltons) between coupled cells. As a result, connexins support the formation of functional cell compartments within tissues, including the bone marrow [27]. The release of CXCL12 requires the close cooperation of stromal cells, which need to function as a network coupled by Cx43 gap junctions [26] (and less so by Cx45). In line with our earlier study [27], we confirmed the close relationship between the stromal L-NGFR

immunoreaction and the Cx43 gap junction plaques by means of protein co-localization. This demonstrated the presence of an intimate connection between the two. The parallel and progressive elevation of their expression suggests that there is an increasing functional activation and potential communication within the stromal network in myelofibrosis, which is in line with the progression of the disease.

In conclusion, all of the growth related biomarkers that we tested, which included L-NGFR, p-ERK1-2, and CXCL12, were likely to be overexpressed in activated bone marrow stromal cells, and their immunoscores were statistically correlated with Gömöri's silver impregnation-based myelofibrosis grades. L-NGFR reaction was restricted to and revealed the entire length of stromal cells, and it showed the best correlations with myelofibrosis grades and had the best overall inter-rater agreements. There is a possibility that compartmental coordination within the myelofibrotic stroma can be supported by the progressive expression of Cx43 gap junctions in the stromal cells. According to the findings of our study, the expression of L-NGFR may be a valuable biological marker of stromal cell activation. As such, it should be given diagnostic consideration as a possible diagnostic complement to Gömöri's silver impregnation. In addition, direct biological evidence of stromal activation will be gained by detecting the expression of various matrix proteins in myelofibrosis. This investigation had been carried out by our group.

In the second part of the study, we focused on extracellular matrix, which has never been studied systematically at the protein level before. We were able to demonstrate, for the first time, that the expression of both type I and type III collagens, as well as fibrillin-1 by bone marrow stromal cells can reveal the extracellular matrix scaffolding in line with the progression of myelofibrosis as classified by Gömöri's silver grading. The traditional grading had the strongest statistical correlations with the uniformly strong firbillin-1 immune signals, which was confirmed by automated whole slide image analysis using an image segmentation algorithm that was based on machine learning. The best correlation was found with the traditional silver impregnation based grading, and the inter-rater agreements were also the strongest with fibrillin-1.

Enhanced matrix accumulation in myelofibrosis is considered to follow the pathway of uncontrolled wound healing as a result of elevated pro-inflammatory cytokine and growth

factor production by aberrant megakaryocytes driven primarily by *JAK2*, *CALR*, or *MPL* mutations through activating the JAK/STAT pathway [68]. This is because elevated pro-inflammatory cytokine and growth factor production by aberrant megakaryocytes is thought to lead to uncontrolled wound healing. The persistent activation of stromal fibroblasts is primarily mediated by transforming growth factor (TGF-β), basic fibroblastic growth factor (bFGF), and platelet-derived growth factor (PDGF) [69] through their cognate receptors. It has been shown that the expression of PDGFR-β is triggered from the early pre-fibrotic phase [23].

We were able to demonstrate that type I and type III collagens, in addition to fibrillin-1, are the primary matrix proteins that constitute the fibrillary scaffold that was revealed by silver impregnation. Because we were able to identify a delicate type III collagen fiber meshwork in early (MF-1) disease samples, we were able to confirm that this protein is involved in the formation of reticular fibers [34-36]. However, the denser fibrillary type I collagen immunoreaction was also revealed at the same time, which suggests that "collagen" fibrosis also begins at the same time. This is in line with the discovery that type III collagen fibrils participate in organizing type I collagen fibrillogenesis [37], which indicates that "collagen" fibrosis also begins at the same time. The reaction with type I collagen showed better correlations with silver grades from the beginning of he fibrosis progression than that with type III collagen. It highlights the fact that "collagen" fibrosis is not only a late event in myelofibrosis but also starts to develop on an earlier stage. These collagen isotypes are confirmed to form separate fibrils by immune electron microscopy, which showed that fibrils with a diameter between 200A and 400A were only positive for type III collagen, whereas fibrils with a diameter greater than 600A were only decorated with type I collagen reaction in skin samples from patients with scleroderma [70]. However, it is possible that fibrils of different isotypes may interact with one another quite closely during the process of collagen fiber formation [37].

Fibrillin-1 immune signal intensities were evenly robust, which offered the best chance out of the three markers to recognize early abnormalities of the stromal scaffolding and matrix deposition in association with myelofibrosis grades. This was because fibrillin-1 immune signal intensities were consistent with one another. Inter-rater agreements, statistical discriminating power between MF-grades of fibrillin-1 reactions, and the

number of cases that were misclassified when compared to Gömöri's silver grading all reflected this fact. In addition, the outcomes of machine learning-based digital image analysis of fibrillin-1 immunoreactions provided strong verification of the findings obtained through eye controlled scoring. The automated analysis also reflected the continuous nature of myelofibrosis progression biology, as shown by the overlapping quant distribution curves of different MF-grades (see Figure 6F). As suggested by knock out (Fbn1-/-) mice osteoblasts showing elevated TGF-β and RANKL (receptor activator of nuclear kappa-B ligand) levels [71, 72], fibrillin-1 microfilaments play essential roles in both the fibrosis of tissue and the remodeling of bone. In a normal situation, the availability of local TGF-β is controlled by fibrillin-1 microfilaments by anchoring it via latent TGF-β binding proteins (LTBPs) [42]. In line with this, congenital dysfunction of fibrillin-1 in scleroderma, also known as stiff skin syndrome, can lead to a high density of type I and type III collagen fiber deposition [73]. This can result in a massive amount of fibrillin-1 that is disorganized. The upregulation of RANKL expression that is caused by TGF-β is a major factor in promoting osteclastogenesis in tissue [72]. Therefore, the upregulated fibrillin-1 expression that we detected with immunostaining in proportion with myelofibrosis grades may reflect a rebound effect aimed at sequestering TGF-β and moderating collagen matrix production. This was found to be in proportion to the severity of the myelofibrosis. Also, fibrillin-1's ability to reduce TGF-β levels can also restrict RANKL production, which in turn inhibits osteoclastogenesis [72]. This may be one factor that contributes to the osteosclerosis that is seen in advanced myelofibrosis. However, in order to prove these ideas, additional confirmation is required.

In contrast to silver impregnation, immunohistochemistry allowed for the examination of normal cell morphology as well as potential functional interactions, such as those between aberrant megakaryocytes and the matrix scaffolding, without the presence of a non-specific background (except rarely for type I collagen, see Figure 9A. inset). In addition, immunohistochemistry made it clear that many clusters of mature red blood cells, which are characteristic of advanced myelofibrosis, had infiltrated the remnants of the matrix network that was located outside of the blood sinuses.

We were able to provide in situ pathobiological evidence of the production and progressive deposition of fibrillary matrix related to stromal cell activation. This evidence

was in line with Gömöri's silver impregnation based grading. "Collagen" fibrosis, which was characterized by type I collagen expression, and "reticulin" fibrosis, which was also characterized by type I collagen expression, were events that occurred in parallel, rather than sequentially. The use of fibrillin-1 immunoreactions enabled an almost perfect visual discrimination between MF-grades at high levels of interobserver agreement, which was supported by image analysis that was based on machine learning. The algorithm separated the visually upgraded and downgraded fibrillin-1 positive cases into the corresponding quant ranges within their original MF-grades. Consequently, in situ detection of these extracellular matrix proteins, in particular fibrillin-1, with or without image analysis can complement diagnostic silver grading of the progression of myelofibrosis at decent structural details.

DOI:10.14753/SE.2023.2889

6 CONCLUSIONS BASED ON NOVEL PUBLISHED OBSERVATIONS

1. Most immunohistochemically detected biomarkers tested in this study showed a significant correlation with the progression of myelofibrosis as characterized by Gömöri's silver impregnation-based grading.

2. Of the stromal growth-related biomarkers tested here, the expression of the low affinity nerve growth factor receptor (L-NGFR; CD271, also referred to as p75) demonstrated the strongest statistical correlation with the Gömöri's silver impregnation based myelofibrosis grading. Therefore, L-NGFR immunohistochemistry may valuably complement silver grading in the rutin diagnostic assessment of primer myelofibrosis progression.

3. Compared to L-NGFR, CXCL12, Phospho-ERK1-2, and Cx43 levels were less accurate indicators of myelofibrosis grades.

4. The glycoprotein fibrillin-1 demonstrated a very strong association with the regular silver impregnation-based grading among the extracellular matrix proteins examined in this study in primary myelofibrotic bone marrow. Since fibrillin-1 was detected throughout stromal cells including their thin processes in addition to its extracellular deposition, fibrillin-1 immunohistochemical detection in primary myelofibrosis is the most promising of the biomarkers evaluated in this study for complementing or even replacing the low reproducibility silver-based grading method.

5. Compared to fibrillin-1, type I and type III collagens were proven to be less accurate myelofibrosis progression indicators compared to Gömöri's silver staining based grading.

6. Using a standardized setup for computer-assisted digital image analysis performed on digital whole slides for fibrillin-1 protein immunostaining resulted in highly reproducible semiquantitative results that statistically strongly correlated with the eye-control based 4 tier (MF0-MF3) of the same digital slides.

.

DOI:10.14753/SE.2023.2889

7 SUMMARY

Status of primary myelofibrosis development is usually evaluated light microscopically and based on Gömöri's silver staining. This semi-quantitative technique calls for seasoned hematopathologists. In addition to evaluation difficulties, standardizing selective silver impregnation preparations is difficult because of the numerous variables that can affect their quality, such as preanalytical circumstances, staining variables, and the absence of an internal positive staining evaluation standard.

The primary objective of the study was to find and determine a good and accurate way to use immunohistochemistry to highlight different growth related markers in bone marrow stromal cells and on matrix components that are related to the fibrogenic process and are eligible to reproduce the traditional three-tier reticulin silver impregnation grading system (Gömöri's staining) in a strong and dependable manner.

First, we analyzed the levels of expression of growth-related biomarkers, including L-NGFR, phospho-ERK1-2, and CXCL12. These biomarkers were primarily detected in the stromal cells of bone marrow, and they play a crucial role in promoting fibroblasts' matrix manufacturing activity. In our studies, it was found that the increasing density of L-NGFR receptor levels had the best correlations with myelofibrosis grades and the best overall agreement between different labs.

In the second part of the study, we focused on matrix proteins such as type I and type III collagens and fibrillin-1. All of the matrix protein immunoreactions that were tested showed close visual and statistical correlations with Gömöri's silver staining in patients with advanced MF-3 myelofibrosis, but fibrillin-1 was the only one that had the strongest correlation within silver-based grade groups at all grade levels.

Statistically significant data suggests that fibrillin-1 staining is a simpler, more standardizable alternative to or possible replacement for the usual silver impregnation-based grading method. We have proved that not only is the correlation with silver staining-based grading significant, but the advantage of high optical contrast also qualifies it for computer-assisted automated image analysis.

8 REFERENCES

[1] Thapa B, Fazal S, Parsi M, Rogers HJ: Myeloproliferative Neoplasms. StatPearls. Treasure Island (FL), 2022.

[2] Garmezy B, Schaefer JK, Mercer J, Talpaz M: A provider's guide to primary myelofibrosis: pathophysiology, diagnosis, and management. Blood Rev 2021, 45:100691.

[3] Moulard O, Mehta J, Fryzek J, Olivares R, Iqbal U, Mesa RA: Epidemiology of myelofibrosis, essential thrombocythemia, and polycythemia vera in the European Union. European Journal of Haematology 2014, 92:289-297.

[4] Titmarsh GJ, Duncombe AS, McMullin MF, O'Rorke M, Mesa R, De Vocht F, Horan S, Fritschi L, Clarke M, Anderson LA: How common are myeloproliferative neoplasms? A systematic review and meta-analysis. American Journal of Hematology 2014, 89:581-587.

[5] Titmarsh GJ, Duncombe AS, McMullin MF, O'Rorke M, Mesa R, De Vocht F, Horan S, Fritschi L, Clarke M, Anderson LA: How common are myeloproliferative neoplasms? A systematic review and meta-analysis. Am J Hematol 2014, 89:581-587.

[6] Tefferi A, Vannucchi AM: Genetic Risk Assessment in Myeloproliferative Neoplasms. Mayo Clin Proc 2017, 92:1283-1290.

[7] Guglielmelli P, Pacilli A, Rotunno G, Rumi E, Rosti V, Delaini F, Maffioli M, Fanelli T, Pancrazzi A, Pietra D, Salmoiraghi S, Mannarelli C, Franci A, Paoli C, Rambaldi A, Passamonti F, Barosi G, Barbui T, Cazzola M, Vannucchi AM: Presentation and outcome of patients with 2016 WHO diagnosis of prefibrotic and overt primary myelofibrosis. Blood 2017, 129:3227-3236.

[8] Emanuel RM, Dueck AC, Geyer HL, Kiladjian JJ, Slot S, Zweegman S, te Boekhorst PA, Commandeur S, Schouten HC, Sackmann F, Kerguelen Fuentes A, Hernández-Maraver D, Pahl HL, Griesshammer M, Stegelmann F, Doehner K, Lehmann T, Bonatz K, Reiter A, Boyer F, Etienne G, Ianotto JC, Ranta D, Roy L, Cahn JY, Harrison CN, Radia D, Muxi P, Maldonado N, Besses C, Cervantes F, Johansson PL, Barbui T, Barosi G, Vannucchi AM, Passamonti F, Andreasson B, Ferrari ML, Rambaldi A, Samuelsson

J, Birgegard G, Tefferi A, Mesa RA: Myeloproliferative neoplasm (MPN) symptom assessment form total symptom score: prospective international assessment of an abbreviated symptom burden scoring system among patients with MPNs. J Clin Oncol 2012, 30:4098-4103.

[9] Tefferi A: Primary myelofibrosis: 2019 update on diagnosis, risk-stratification and management. American Journal of Hematology 2018, 93:1551-1560.

[10] Abdallah Abou Z, Mohamed ES, Nicole C, Douglas T, Srdan V, Ruben M, Ronald H, John M: Bone marrow fibrosis in myelofibrosis: pathogenesis, prognosis and targeted strategies. Haematologica 2016, 101:660-671.

[11] Szekely T, Krenacs T, Maros ME, Bodor C, Daubner V, Csizmadia A, Vrabely B, Timar B: Correlations Between the Expression of Stromal Cell Activation Related Biomarkers, L-NGFR, Phospho-ERK1-2 and CXCL12, and Primary Myelofibrosis Progression. Pathology and Oncology Research 2022, 28.

[12] Gangat N, Caramazza D, Vaidya R, George G, Begna K, Schwager S, Van Dyke D, Hanson C, Wu W, Pardanani A, Cervantes F, Passamonti F, Tefferi A: DIPSS plus: a refined Dynamic International Prognostic Scoring System for primary myelofibrosis that incorporates prognostic information from karyotype, platelet count, and transfusion status. J Clin Oncol 2011, 29:392-397.

[13] Gangat N, Caramazza D, Vaidya R, George G, Begna K, Schwager S, Van Dyke D, Hanson C, Wu W, Pardanani A: DIPSS plus: a refined Dynamic International Prognostic Scoring System for primary myelofibrosis that incorporates prognostic information from karyotype, platelet count, and transfusion status. Journal of Clinical Oncology 2011, 29:392-397.

[14] Cattoretti G, Schiró R, Orazi A, Soligo D, Colombo MP: Bone marrow stroma in humans: anti-nerve growth factor receptor antibodies selectively stain reticular cells in vivo and in vitro. Blood 1993, 81:1726-1738.

[15] Covaceuszach S, Konarev PV, Cassetta A, Paoletti F, Svergun DI, Lamba D, Cattaneo A: The conundrum of the high-affinity NGF binding site formation unveiled? Biophysical journal 2015, 108:687-697.

[16] Micera A, Lambiase A, Stampachiacchiere B, Bonini S, Bonini S, Levi-Schaffer F: Nerve growth factor and tissue repair remodeling: trkA(NGFR) and p75(NTR), two receptors one fate. Cytokine & growth factor reviews 2007, 18:245-256.

[17] Barilani M, Banfi F, Sironi S, Ragni E, Guillaumin S, Polveraccio F, Rosso L, Moro M, Astori G, Pozzobon M, Lazzari L: Low-affinity Nerve Growth Factor Receptor (CD271) Heterogeneous Expression in Adult and Fetal Mesenchymal Stromal Cells. Scientific reports 2018, 8:9321.

[18] Tomlinson RE, Li Z, Zhang Q, Goh BC, Li Z, Thorek DLJ, Rajbhandari L, Brushart TM, Minichiello L, Zhou F, Venkatesan A, Clemens TL: NGF-TrkA Signaling by Sensory Nerves Coordinates the Vascularization and Ossification of Developing Endochondral Bone. Cell reports 2016, 16:2723-2735.

[19] Zheng MG, Sui WY, He ZD, Liu Y, Huang YL, Mu SH, Xu XZ, Zhang JS, Qu JL, Zhang J, Wang D: TrkA regulates the regenerative capacity of bone marrow stromal stem cells in nerve grafts. Neural regeneration research 2019, 14:1765-1771.

[20] Bock O, Loch G, Büsche G, von Wasielewski R, Schlué J, Kreipe H: Aberrant expression of platelet-derived growth factor (PDGF) and PDGF receptor-alpha is associated with advanced bone marrow fibrosis in idiopathic myelofibrosis. Haematologica 2005, 90:133-134.

[21] Bedekovics J, Kiss A, Beke L, Károlyi K, Méhes G: Platelet derived growth factor receptor-beta (PDGFRβ) expression is limited to activated stromal cells in the bone marrow and shows a strong correlation with the grade of myelofibrosis. Virchows Archiv : an international journal of pathology 2013, 463:57-65.

[22] Bedekovics J, Szeghalmy S, Beke L, Fazekas A, Méhes G: Image analysis of platelet derived growth factor receptor-beta (PDGFRβ) expression to determine the grade and dynamics of myelofibrosis in bone marrow biopsy samples. Cytometry Part B, Clinical cytometry 2014, 86:319-328.

[23] Méhes G, Tzankov A, Hebeda K, Anagnostopoulos I, Krenács L, Bedekovics J: Platelet-derived growth factor receptor β (PDGFRβ) immunohistochemistry highlights activated bone marrow stroma and is potentially predictive for fibrosis progression in prefibrotic myeloproliferative neoplasia. Histopathology 2015, 67:617-624.

[24] Kitagawa M, Kurata M, Onishi I, Yamamoto K: Bone marrow niches in myeloid neoplasms. Pathology international 2020, 70:63-71.

[25] Singh P, Mohammad KS, Pelus LM: CXCR4 expression in the bone marrow microenvironment is required for hematopoietic stem and progenitor cell maintenance and early hematopoietic regeneration after myeloablation. Stem cells (Dayton, Ohio) 2020, 38:849-859.

[26] Schajnovitz A, Itkin T, D'Uva G, Kalinkovich A, Golan K, Ludin A, Cohen D, Shulman Z, Avigdor A, Nagler A, Kollet O, Seger R, Lapidot T: CXCL12 secretion by bone marrow stromal cells is dependent on cell contact and mediated by connexin-43 and connexin-45 gap junctions. Nature immunology 2011, 12:391-398.

[27] Krenacs T, Rosendaal M: Connexin43 gap junctions in normal, regenerating, and cultured mouse bone marrow and in human leukemias: their possible involvement in blood formation. The American journal of pathology 1998, 152:993-1004.

[28] Abdelouahab H, Zhang Y, Wittner M, Oishi S, Fujii N, Besancenot R, Plo I, Ribrag V, Solary E, Vainchenker W, Barosi G, Louache F: CXCL12/CXCR4 pathway is activated by oncogenic JAK2 in a PI3K-dependent manner. Oncotarget 2017, 8:54082-54095.

[29] López-Gil JC, Martin-Hijano L, Hermann PC, Sainz B, Jr.: The CXCL12 Crossroads in Cancer Stem Cells and Their Niche. Cancers 2021, 13.

[30] Schepers K, Pietras EM, Reynaud D, Flach J, Binnewies M, Garg T, Wagers AJ, Hsiao EC, Passegué E: Myeloproliferative neoplasia remodels the endosteal bone marrow niche into a self-reinforcing leukemic niche. Cell stem cell 2013, 13:285-299.

[31] Hochweiss S, Fruchtman S, Hahn EG, Gilbert H, Donovan PB, Johnson J, Goldberg JD, Berk PD: Increased serum procollagen III aminoterminal peptide in myelofibrosis. Am J Hematol 1983, 15:343-351.

[32] Lisse I, Hasselbalch H, Junker P: Bone marrow stroma in idiopathic myelofibrosis and other haematological diseases. An immunohistochemical study. Apmis 1991, 99:171-178.

[33] Henriksen K, Karsdal MA: Chapter 1 - Type I collagen. Biochemistry of Collagens, Laminins and Elastin (Second Edition). Edited by Karsdal MA. Academic Press, 2019. pp. 1-12.

[34] Kuivaniemi H, Tromp G: Type III collagen (COL3A1): Gene and protein structure, tissue distribution, and associated diseases. Gene 2019, 707:151-171.

[35] Unsworth DJ, Scott DL, Almond TJ, Beard HK, Holborow EJ, Walton KW: Studies on reticulin. I: Serological and immunohistological investigations of the occurrence of collagen type III, fibronectin and the non-collagenous glycoprotein of Pras and Glynn in reticulin. Br J Exp Pathol 1982, 63:154-166.

[36] Glegg RE, Eidinger D, Leblond CP: Some carbohydrate components of reticular fibers. Science 1953, 118:614-616.

[37] Liu X, Wu H, Byrne M, Krane S, Jaenisch R: Type III collagen is crucial for collagen I fibrillogenesis and for normal cardiovascular development. Proc Natl Acad Sci U S A 1997, 94:1852-1856.

[38] Lin X, Patil S, Gao YG, Qian A: The Bone Extracellular Matrix in Bone Formation and Regeneration. Front Pharmacol 2020, 11:757.

[39] Kvasnicka HM, Beham-Schmid C, Bob R, Dirnhofer S, Hussein K, Kreipe H, Kremer M, Schmitt-Graeff A, Schwarz S, Thiele J, Werner M, Stein H: Problems and pitfalls in grading of bone marrow fibrosis, collagen deposition and osteosclerosis - a consensus-based study. Histopathology 2016, 68:905-915.

[40] Thomson J, Singh M, Eckersley A, Cain SA, Sherratt MJ, Baldock C: Fibrillin microfibrils and elastic fibre proteins: Functional interactions and extracellular regulation of growth factors. Semin Cell Dev Biol 2019, 89:109-117.

[41] Jensen SA, Handford PA: New insights into the structure, assembly and biological roles of 10-12 nm connective tissue microfibrils from fibrillin-1 studies. Biochem J 2016, 473:827-838.

[42] Olivieri J, Smaldone S, Ramirez F: Fibrillin assemblies: extracellular determinants of tissue formation and fibrosis. Fibrogenesis Tissue Repair 2010, 3:24.

[43] Arber DA, Orazi A, Hasserjian R, Thiele J, Borowitz MJ, Le Beau MM, Bloomfield CD, Cazzola M, Vardiman JW: The 2016 revision to the World Health Organization classification of myeloid neoplasms and acute leukemia. Blood 2016, 127:2391-2405.

[44] Gömöri G: Silver Impregnation of Reticulum in Paraffin Sections. The American journal of pathology 1937, 13:993-1002.5.

[45] Thiele J, Kvasnicka HM, Facchetti F, Franco V, van der Walt J, Orazi A: European consensus on grading bone marrow fibrosis and assessment of cellularity. Haematologica 2005, 90:1128-1132.

[46] Szekely T, Krenacs T, Maros ME, Bodor C, Daubner V, Csizmadia A, Vrabely B, Timar B: Correlations Between the Expression of Stromal Cell Activation Related Biomarkers, L-NGFR, Phospho-ERK1-2 and CXCL12, and Primary Myelofibrosis Progression. Pathol Oncol Res 2022, 28:1610217.

[47] Maros ME, Wenz R, Förster A, Froelich MF, Groden C, Sommer WH, Schönberg SO, Henzler T, Wenz H: Objective Comparison Using Guideline-based Query of Conventional Radiological Reports and Structured Reports. In vivo (Athens, Greece) 2018, 32:843-849.

[48] Szekely T, Wichmann B, Maros ME, Csizmadia A, Bodor C, Timar B, Krenacs T: Myelofibrosis progression grading based on type I and type III collagen and fibrillin 1 expression boosted by whole slide image analysis. Histopathology 2022.

[49] Tefferi A: Primary myelofibrosis: 2019 update on diagnosis, risk-stratification and management. Am J Hematol 2018, 93:1551-1560.

[50] Schieber M, Crispino JD, Stein B: Myelofibrosis in 2019: moving beyond JAK2 inhibition. Blood cancer journal 2019, 9:74.

[51] Barbui T, Thiele J, Gisslinger H, Kvasnicka HM, Vannucchi AM, Guglielmelli P, Orazi A, Tefferi A: The 2016 WHO classification and diagnostic criteria for myeloproliferative neoplasms: document summary and in-depth discussion. Blood cancer journal 2018, 8:15.

[52] Canossa M, Twiss JL, Verity AN, Shooter EM: p75(NGFR) and TrkA receptors collaborate to rapidly activate a p75(NGFR)-associated protein kinase. The EMBO journal 1996, 15:3369-3376.

[53] Barker PA: p75NTR: A study in contrasts. Cell death and differentiation 1998, 5:346-356.

[54] Casaccia-Bonnefil P, Kong H, Chao MV: Neurotrophins: the biological paradox of survival factors eliciting apoptosis. Cell death and differentiation 1998, 5:357-364.

[55] Labouyrie E, Dubus P, Groppi A, Mahon FX, Ferrer J, Parrens M, Reiffers J, de Mascarel A, Merlio JP: Expression of neurotrophins and their receptors in human bone marrow. The American journal of pathology 1999, 154:405-415.

[56] Zha K, Yang Y, Tian G, Sun Z, Yang Z, Li X, Sui X, Liu S, Zhao J, Guo Q: Nerve growth factor (NGF) and NGF receptors in mesenchymal stem/stromal cells: Impact on potential therapies. Stem cells translational medicine 2021, 10:1008-1020.

[57] García R, Aguiar J, Alberti E, de la Cuétara K, Pavón N: Bone marrow stromal cells produce nerve growth factor and glial cell line-derived neurotrophic factors. Biochemical and biophysical research communications 2004, 316:753-754.

[58] Caneva L, Soligo D, Cattoretti G, De Harven E, Deliliers GL: Immuno-electron microscopy characterization of human bone marrow stromal cells with anti-NGFR antibodies. Blood cells, molecules & diseases 1995, 21:73-85.

[59] Calabrese G, Giuffrida R, Lo Furno D, Parrinello NL, Forte S, Gulino R, Colarossi C, Schinocca LR, Giuffrida R, Cardile V, Memeo L: Potential Effect of CD271 on Human Mesenchymal Stromal Cell Proliferation and Differentiation. International journal of molecular sciences 2015, 16:15609-15624.

[60] Quirici N, Soligo D, Bossolasco P, Servida F, Lumini C, Deliliers GL: Isolation of bone marrow mesenchymal stem cells by anti-nerve growth factor receptor antibodies. Experimental hematology 2002, 30:783-791.

[61] Yigit N, Covey S, Barouk-Fox S, Turker T, Geyer JT, Orazi A: Nuclear factor-erythroid 2, nerve growth factor receptor, and CD34-microvessel density are differentially expressed in primary myelofibrosis, polycythemia vera, and essential thrombocythemia. Human pathology 2015, 46:1217-1225.

[62] Beyer C, Distler JH: Tyrosine kinase signaling in fibrotic disorders: Translation of basic research to human disease. Biochimica et biophysica acta 2013, 1832:897-904.

[63] Satomura K, Derubeis AR, Fedarko NS, Ibaraki-O'Connor K, Kuznetsov SA, Rowe DW, Young MF, Gehron Robey P: Receptor tyrosine kinase expression in human bone marrow stromal cells. Journal of cellular physiology 1998, 177:426-438.

[64] Dupree MA, Pollack SR, Levine EM, Laurencin CT: Fibroblast growth factor 2 induced proliferation in osteoblasts and bone marrow stromal cells: a whole cell model. Biophysical journal 2006, 91:3097-3112.

[65] Pagès G, Lenormand P, L'Allemain G, Chambard JC, Meloche S, Pouysségur J: Mitogen-activated protein kinases p42mapk and p44mapk are required for fibroblast proliferation. Proc Natl Acad Sci U S A 1993, 90:8319-8323.

[66] Plotnikov A, Zehorai E, Procaccia S, Seger R: The MAPK cascades: signaling components, nuclear roles and mechanisms of nuclear translocation. Biochimica et biophysica acta 2011, 1813:1619-1633.

[67] Song MK, Park BB, Uhm JE: Understanding Splenomegaly in Myelofibrosis: Association with Molecular Pathogenesis. International journal of molecular sciences 2018, 19.

[68] Savona MR: Are we altering the natural history of primary myelofibrosis? Leuk Res 2014, 38:1004-1012.

[69] Agarwal A, Morrone K, Bartenstein M, Zhao ZJ, Verma A, Goel S: Bone marrow fibrosis in primary myelofibrosis: pathogenic mechanisms and the role of TGF-β. Stem Cell Investig 2016, 3:5.

[70] Fleischmajer R, Gay S, Perlish JS, Cesarini JP: Immunoelectron microscopy of type III collagen in normal and scleroderma skin. J Invest Dermatol 1980, 75:189-191.

[71] Godwin ARF, Singh M, Lockhart-Cairns MP, Alanazi YF, Cain SA, Baldock C: The role of fibrillin and microfibril binding proteins in elastin and elastic fibre assembly. Matrix Biol 2019, 84:17-30.

[72] Nistala H, Lee-Arteaga S, Smaldone S, Siciliano G, Ramirez F: Extracellular microfibrils control osteoblast-supported osteoclastogenesis by restricting TGF{beta} stimulation of RANKL production. J Biol Chem 2010, 285:34126-34133.

DOI:10.14753/SE.2023.2889

[73] Gabrielli A, Avvedimento EV, Krieg T: Scleroderma. N Engl J Med 2009, 360:1989-2003.

9 BIBLIOGRAPHY OF THE CANDIDATE'S PUBLICATIONS

Total of impact factors: 17.283

Publications related to PhD dissertation *(subtotal of impact factors: 10.652)*

Szekely T, Krenacs T, Maros ME, Bodor C, Daubner V, Csizmadia A, Vrabely B, Timar B: Correlations Between the Expression of Stromal Cell Activation Related Biomarkers, L-NGFR, Phospho-ERK1-2 and CXCL12, and Primary Myelofibrosis Progression. Pathol Oncol Res 2022, 28:1610217. *(journals's impact factor in 2022 : 2.874)*

Szekely T, Wichmann B, Maros ME, Csizmadia A, Bodor C, Timar B, Krenacs T: Myelofibrosis progression grading based on type I and type III collagen and fibrillin 1 expression boosted by whole slide image analysis. Histopathology 2022 *(journals's impact factor in 2022 : 7.778)*

Additional papers not related to the PhD thesis *(subtotal of impact factors: 6.631)*

Krenacs, T., Meggyeshazi, N., Forika, G., Kiss, E., Hamar, P., Szekely, T., & Vancsik, T. (2020). Modulated Electro-Hyperthermia-Induced Tumor Damage Mechanisms Revealed in Cancer Models. International journal of molecular sciences, 21(17), 6270. https://doi.org/10.3390/ijms21176270 *(journals's impact factor in 2020 : 5.924)*

Fónyad, L., & Székely, T. (2021). Online patológiai vizsgálatkérő felület létrehozása a Semmelweis Egyetemen [Online pathology request platform at the Semmelweis University]. Orvosi hetilap, 162(49), 1962–1967. https://doi.org/10.1556/650.2021.32306 *(journals's impact factor in 2021 : 0.707)*

DOI:10.14753/SE.2023.2889

10 ACKNOWLEDGEMENTS

I am grateful to Prof. Tibor Krenács for providing the opportunity to work in his laboratory and for constantly supervising my work.

I am thankful to Prof. András Matolcsy for letting me work in his institution and for letting me study in the Pathology Doctoral School.

I am thankful to Botond Timár for helping with sample collection, evaluation, and explaining me various hematopathological aspects of the topic in details.

I am grateful to all the members of the laboratory, especially Eva Mátrainé Balogh, for their excellent technical support in the laboratory work.

I am grateful to Máté Maros and Barna Wichmann for their excellent support in statistical analysis laboratory work.

I am also grateful to all members of the Department of Pathology and Experimental Cancers Research at Semmelweis University who helped me in any aspect of my studies.

Finally, but not least, I am truly grateful to my beloved family and friends, who give me a stable background and motivation throughout my work.